AD-A091 543 AIR FORCE WRIGHT AERONAUTICAL LABS WRIGHT-PATTERSON AFB OH F/G 14/2
EFFECTS OF DOWNSTREAM DISTANCE ON TURBULENCE DECAY FOR THE COMP--ETC(U)
MAR 80 D C RABE

UNCLASSIFIED AFWAL-TR-80-2023 NL

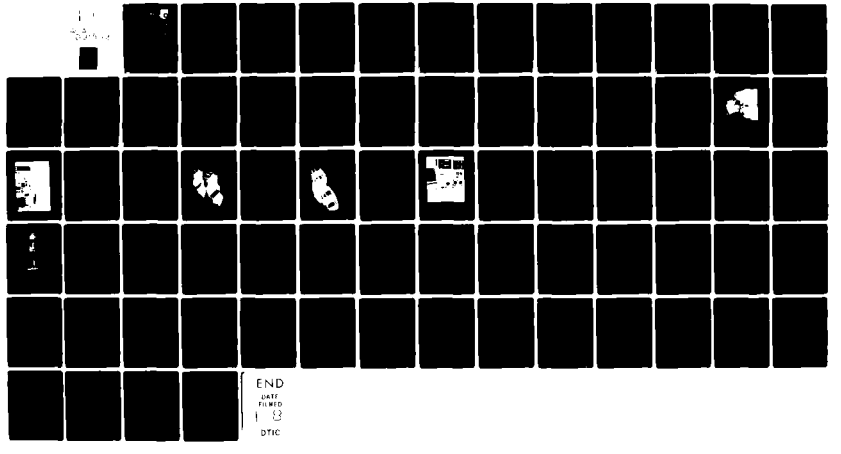

END
DATE FILMED
8
DTIC

(14) AFWAL-TR-80-2023

LEVEL II

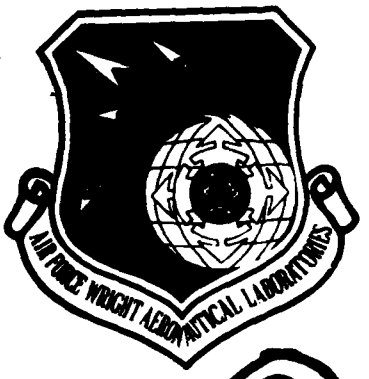

AD A091543

(2)

(6) EFFECTS OF DOWNSTREAM DISTANCE ON TURBULENCE DECAY FOR THE COMPRESSOR RESEARCH FACILITY FLOW CONDITIONING SYSTEM

(10) Douglas C. Rabe
Technology Branch
Turbine Engine Division

DTIC
ELECTE
NOV 13 1980
S D
E

(12) 72

(11) March 1980

(9) TECHNICAL REPORT AFWAL-TR-80-2023
Final Report, ~~for the Period~~ 1 Feb~~ruary~~ 19~~78~~ ~~to~~ 1 July 1979

(16) 3066

(17) 17

Approved for public release; distribution unlimited

AERO PROPULSION LABORATORY
AIR FORCE WRIGHT AERONAUTICAL LABORATORIES
AIR FORCE SYSTEMS COMMAND
WRIGHT-PATTERSON AIR FORCE BASE, OHIO 45433

DDC FILE COPY

392662

80 10 31 065

62203F

NOTICE

When Government drawings, specifications, or other data are used for any purpose other than in connection with a definitely related Government procurement operation, the United States Government thereby incurs no responsibility nor any obligation whatsoever; and the fact that the government may have formulated, furnished, or in any way supplied the said drawings, specifications, or other data, is not to be regarded by implication or otherwise as in any manner licensing the holder or any other person or corporation, or conveying any rights or permission to manufacture use, or sell any patented invention that may in any way be related thereto.

This report has been reviewed by the Office of Public Affairs (ASD/PA) and is releasable to the National Technical Information Service (NTIS). At NTIS, it will be available to the general public, including foreign nations.

This technical report has been reviewed and is approved for publication.

DOUGLAS C. RABE
Aerospace Engineer
Compressor Test Group
Technology Branch

DR. FRANCIS R. OSTDIEK
Chief, Compressor Test Group
Technology Branch

FOR THE COMMANDER

H. I. BUSH, Deputy Director
Turbine Engine Division
Aero Propulsion Laboratory

"If your address has changed, if you wish to be removed from our mailing list, or if the addressee is no longer employed by your organization please notify AFWAL/POTX, *W-PAFB, OH 45433 to help us maintain a current mailing list".*

Copies of this report should not be returned unless return is required by security considerations, contractual obligations, or notice on a specific document.

SECURITY CLASSIFICATION OF THIS PAGE (When Data Entered)

REPORT DOCUMENTATION PAGE

READ INSTRUCTIONS BEFORE COMPLETING FORM

1. REPORT NUMBER: AFWAL-TR-80-2023 ✓	2. GOVT ACCESSION NO.: AD-A091 543
3. RECIPIENT'S CATALOG NUMBER:	
4. TITLE (and Subtitle): Effects of Downstream Distance on Turbulence Decay for the Compressor Research Facility Flow Conditioning System	5. TYPE OF REPORT & PERIOD COVERED: Final Report 1 February 78 to 1 July 79
	6. PERFORMING ORG. REPORT NUMBER:
7. AUTHOR(s):	8. CONTRACT OR GRANT NUMBER(s):
9. PERFORMING ORGANIZATION NAME AND ADDRESS: Aero Propulsion Laboratory (POTX) ✓ Air Force Wright Aeronautical Laboratories, AFSC Wright-Patterson Air Force Base, Ohio 45433	10. PROGRAM ELEMENT, PROJECT, TASK AREA & WORK UNIT NUMBERS: Program Element - 646100 Project-3066, Task-306617 Work Unit- 30661740
11. CONTROLLING OFFICE NAME AND ADDRESS: Aero Propulsion Laboratory (POTX) Air Force Wright Aeronautical Laboratories, AFSC Wright-Patterson Air Force Base, Ohio 45433	12. REPORT DATE: March 1980
	13. NUMBER OF PAGES: 71
14. MONITORING AGENCY NAME & ADDRESS (if different from Controlling Office):	15. SECURITY CLASS. (of this report): UNCLASSIFIED
	15a. DECLASSIFICATION/DOWNGRADING SCHEDULE:

16. DISTRIBUTION STATEMENT (of this Report)

Approved for public release; distribution unlimited.

17. DISTRIBUTION STATEMENT (of the abstract entered in Block 20, if different from Report)

18. SUPPLEMENTARY NOTES

19. KEY WORDS (Continue on reverse side if necessary and identify by block number)

Turbulence decay
Turbulence

20. ABSTRACT (Continue on reverse side if necessary and identify by block number)

The turbulence decay of the 304.8 cm. (120 in.) diameter flow conditioning system for the Air Force Aero Propulsion Laboratory's Compressor Research Facility was investigated in a 25.4 cm. (10 in.) diameter channel to predict turbulence levels that can be expected at the entrance to compressors being tested in the facility. Results of this experimentation show that the flow conditioning system will meet the design goal of reducing the expected incoming turbulence level of 30-40% to less than 1% at the entrance to a test

DD FORM 1 JAN 73 1473 EDITION OF 1 NOV 65 IS OBSOLETE

SECURITY CLASSIFICATION OF THIS PAGE (When Data Entered)

compressor. Further, the turbulence decay associated with the full-flow conditioning system and its individual components possesses initial period of decay characteristics throughout the 600 cm. decay length investigated. It is concluded that these decay characteristics are due to the large scale of turbulence incoming and exiting the flow conditioning system of the Compressor Research Facility.

FOREWORD

This report contains the results of a thesis prepared for the Aeronautical and Astronautical Engineering Department of the Ohio State University. The effort was performed in the Technology Branch of the Turbine Engine Division of the Air Force Aero Propulsion Laboratory, Air Force Systems Command, Wright-Patterson AFB, Ohio, under Project 3066, Task 306617 and Work Unit 30661740. A one-tenth scale flow channel was constructed to simulate a stream tube of the Compressor Research Facility flow conditioning system. Turbulence decay was then measured throughout the full scale flow distance of the Compressor Research Facility to determine the turbulence level that can be expected at the entrance to test compressors.

This effort was conducted by Douglas C. Rabe during the period February 1978 to July 1979.

TABLE OF CONTENTS

LIST OF ILLUSTRATIONS

LIST OF ILLUSTRATIONS

LIST OF SYMBOLS

SYMBOL	DESCRIPTION
A	Arbitrary constant
a	Radius of the channel
B	Arbitrary constant
dw	Diameter of the hot wire
E	Mean (DC) voltage of the hot wire
E^1	Mean kinetic energy of turbulence per unit volume
E_1^1	Mean kinetic energy of turbulence per unit volume upstream of a flow conditioning element
E_2^1	Mean kinetic energy of turbulence per unit volume downstream of a flow conditioning element
e^1	Root-mean-square value of the fluctuating (AC) voltage of the hot wire
f	Turbulence reduction factor
f_1	Longitudinal turbulence reduction factor
fuv	Longitudinal and lateral turbulence reduction factor
Gr	Grashof number
H_f	Heat transfer coefficient from hot wire to fluid
K	Pressure drop coefficient
K_f	Thermal conductivity of the fluid
L	Nondimensional inlet length
ℓw	Length of the hot wire
m	Arbitrary constant
Nu	Nusselt number
n	Number of screens

LIST OF SYMBOLS (Cont'd)

SYMBOL	DESCRIPTION
PO	Total pressure
PS	Static pressure
ΔP	Pressure drop across a flow conditioning element
R_e	Reynolds Number
Tf	Static temperature of the fluid
Tm	Mean Temperature = 1/2(Tw+Tf)
Tw	Static temperature of the hot wire
t	Time for turbulence decay
U	Mean velocity
u^1	Root-mean-square of the fluctuations of axial velocity
u_1	Fluctuating velocity in the axial direction upstream of a flow conditioning element
u_3	Fluctuating velocity in the axial direction downstream of a flow conditioning element
v_1	Fluctuating velocity in the radial direction upstream of a flow conditioning element
v_3	Fluctuating velocity in the radial direction downstream of a flow conditioning element
x	Distance down the channel
α	Limiting value of the ratio of the exit flow angle to the incident flow angle as the incident flow angle approaches zero. The angles are measured with respect to the flow conditioning element normal.
ρ	Density
τ	Turbulence level in percent = $u^1/U \times 100\%$
μ	Kinematic viscosity of the fluid
μ_f	Kinematic viscosity of the fluid evaluated at Tm

I. INTRODUCTION

In the aircraft gas turbine industry, past experience shows that compressors and fans go through from two to eight redesigns before reaching operational status. Many of the compressors that do become operational go through further redesigns in an attempt to improve their performance. The cost of these redesigns can be staggering, ranging into the tens of millions of dollars.

Because of these costs and associated program delays, the Air Force has decided to construct the Compressor Research Facility (CRF). The facility will enable the government to investigate both steady-state and transient jet engine compressor performance. In order to obtain transient compressor performance data, the facility is totally computer controlled. In addition, data is acquired and digitized at a rate of 100,000 samples/sec.

The inlet air system for the Compressor Research Facility is shown in Figure 1. To simulate flight conditions at elevated altitudes, and/or to reduce power requirements, the test compressor is mounted inside an 18.3 by 6.1 meter test chamber. Using a series of five inlet control valves (three shown in Figure 1) and a discharge valve, the tank pressure and/or mass flow can be regulated. A mass flow from 6.8 to 226.8 Kg./sec. can be accommodated through the test chamber with a minimum allowable static pressure in the test chamber of .14 atmosphere which corresponds to an altitude of 14173.0 meters. The compressor itself provides the exhauster capability for the facility. A test compressor can be driven by either a 22.4 Megawatt electric motor

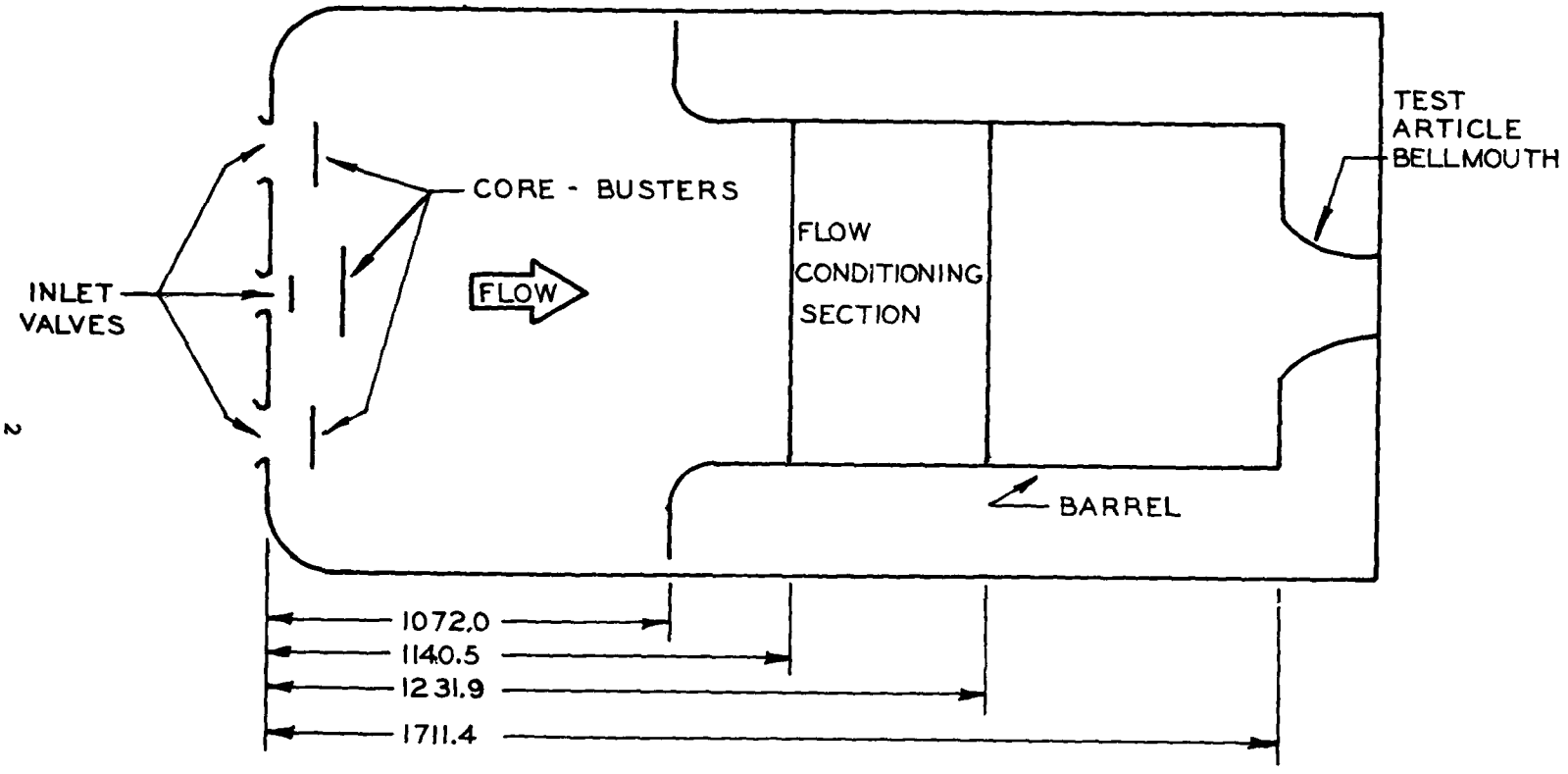

FIGURE 1 CROSS SECTION OF THE CRF TEST CHAMBER WITH BARREL DIMENSIONS IN CENTIMETERS

which can rotate the test article at a maximum speed of 15,000 RPM or an 11.2 Megawatt electric motor which can rotate the test article to a maximum speed of 30,000 RPM.

In order to make valid comparisons of performance between compressors, the compressor efficiencies must be determined to an accuracy of better than 1%. To accurately establish compressor characteristics, the flow quality standards should be chosen to represent the minimum flow conditions that will affect compressor performance or surge margin. Recommendations for the Compressor Research Facility flow quality standards have been reported previously.[1 & 2] One of these recommended flow quality standards is a turbulence level at the inlet to the test compressor of less than 1%. The turbulence level is defined as the percentage of the root-mean-square of the axial fluctuation of velocity, u^1, to the average value of axial velocity, U, as shown in Equation (1).

$$\tau = \frac{u^1}{U} \times 100\% \qquad (1)$$

Using hot wire anemometers in a 1/10th scale model of the Compressor Research Facility inlet flow system, previous unpublished work by Ostdiek and Rivir[3] determined a method of reducing the incoming turbulence level of 40 - 60% to an acceptable level. This reduction in turbulence was accomplished by investigating a number of flow conditioning systems and proposing a final configuration described in Reference 4. However, due to practical limitations, measurements of the turbulence level in the scale model were made without the decay length of 476 cm. found in the actual facility.

For mechanical reasons, the flow conditioning system previously recommended[3] has been changed, and the final design of the Compressor Research Facility flow conditioning system is shown in Figure 2 while Figure 1 shows its relationship within the facility's inlet air system. The present flow conditioner was made as two conditioning units in order to distribute its weight more evenly over the test chamber. Further, since stalls and surges are to be investigated in the facility, the support grids appear on both the upstream and downstream sides of both conditioning units to support the turbulence reducing screens for flow in both directions. The large wire diameter screen located on the downstream side of the conditioning system is designed to reduce incoming turbulence at low velocities while the smaller diameter wire screens are designed to reduce incoming turbulence at the higher velocities. The honeycomb sections are designed for a length to diameter ratio on the order of 20:1 to meet directional flow quality standards.

The changes in the present flow conditioning system to what has been previously investigated,[3 & 4] as well as the importance of the test facility, make it highly desirable to investigate the effects of downstream distance on turbulence decay for the present flow conditioning system and its components.

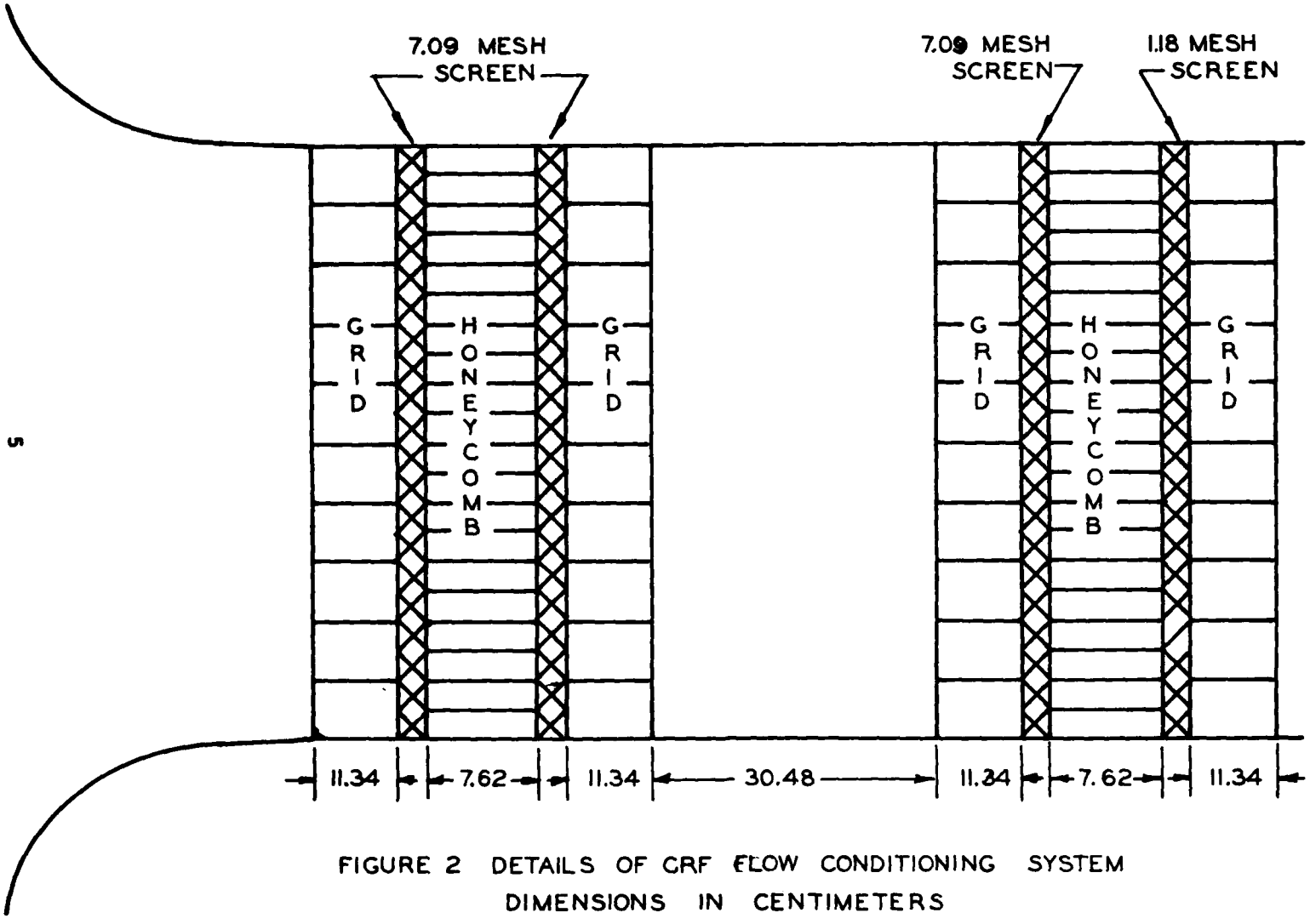

FIGURE 2 DETAILS OF GRF FLOW CONDITIONING SYSTEM
DIMENSIONS IN CENTIMETERS

II. BACKGROUND

Turbulence decay has been previously studied by many authors. Batchelor and Townsend[5 & 6], in two reports, studied both the initial and final periods of decay behind screens. The incoming turbulence level in these studies was less than 1% and was considered isotropic where isotropic turbulence possesses the characteristic that the three components of fluctuating velocity have the same magnitude. It was found that the initial period of decay behaved according to

$$\overline{u^2} \propto t^{-1} \tag{2}$$

where t is the time for decay. During the initial period of decay, the viscous and inertia forces are of comparable importance. After a transition period which begins at approximately 150 mesh lengths downstream of the screen, turbulence reduction tends towards what is called the final period of decay. In the final period inertial forces become negligible and turbulence reduction is predominated by viscous forces and follows the characteristics of

$$\overline{u^2} \propto t^{-5/2} \tag{3}$$

Subsequent work by Schubauer, Spangenberg and Klebanoff[7] experimentally investigated four previously proposed empirical theories of turbulence reduction. These theories relate the turbulence reduction factor f, defined as the ratio of the turbulence level found after the flow has passed through a screen to the turbulence level at the same point in the absence of the screen, as a function of the screen pressure drop. Defining the pressure-drop coefficient K in terms of the screen pressure drop ΔP as

$$K = \frac{\Delta P}{1/2 e U^2} \tag{4}$$

the four empirical theories can be summarized as follows:

Prandtl $$f_1 = \frac{1}{1+K} \tag{5}$$

Collar $$f_1 = \frac{2-K}{2+K} \tag{6}$$

Taylor and Batchelor $$f_1 = \frac{1+\alpha-\alpha K}{1+\alpha+K} \tag{7}$$

Dryden and Schubauer $$fuv = \left(\frac{1}{1+K}\right)^{1/2} \tag{8}$$

Of the four theories, Prandtl, Collar and Taylor and Batchelor distinguish f_1 as the longitudinal turbulence reduction factor where fuv in the Dryden and Schubauer theory is the reduction factor for either the longitudinal or lateral turbulent energy.

It can also be shown that Equation (7) reduces to Equation (5) when $\alpha = 0$ and to Equation (6) when $\alpha = 1$. The value of α is defined in terms of flow angles measured with respect to the screen normal and is the limiting value of the exit flow angle to the incident flow angle as the incident angle approaches zero. Therefore, the Prandtl theory would be useful for screens of high solidity and the Collar theory for screens of low solidity while the Taylor and Batchelor and Dryden and Schubauer theories are more general.

The experimental investigation[7] of the applicability of the four theories for turbulence decay was conducted in air with an incoming turbulence level on the order of 1%. Again, as in Batchelor and Townsend,[5 & 6] only screens were investigated, and the incoming turbulence could be considered isotropic. Their investigation concluded that when the velocity equalled or exceeded the value necessary for the initial shedding of eddies by the screen, the longitudinal and lateral turbulence was reduced as the theory of Dryden and Schubauer predicted [Equation (8)].

In their report, Dryden and Schubauer[8] derived the reduction factor for longitudinal and lateral turbulence. During their derivation, it was assumed that the change in the mean kinetic energy of turbulence per unit volume would occur only on the upstream side of the screen. Thus, the mean kinetic energy of turbulence per unit volume loss due to the screen KE_3^1 was written

$$KE_3^1 = E_1^1 - E_3^1 \tag{9}$$

where E_1^1 and E_3^1 are the values of the mean kinetic energy of turbulence per unit volume upstream and downstream, respectively, of the screen. From Equation (9) the ratio of downstream to upstream turbulent kinetic energy can be written as

$$\frac{E_3^1}{E_1^1} = \frac{1}{1+K} \tag{10}$$

Since the mean kinetic energy of turbulence per unit volume for the axisymmetric case is

$$E^1 = 1/2\rho\left(\overline{u^2} + \overline{v^2}\right) \tag{11}$$

a turbulence reduction factor across one screen can be defined as

$$fuv = \left(\frac{\overline{u_1^2} + \overline{v_1^2}}{\overline{u_3^2} + \overline{v_3^2}}\right)^{1/2} \tag{12}$$

For isotropic turbulence where $u_1 = v_1$ and $u_3 = v_3$, f would become the previously discussed turbulence reduction factor independent of direction and would be

$$fuv = \left(\frac{E_3^1}{E_1^1}\right)^{1/2} = \left(\frac{1}{1+K}\right)^{1/2} \tag{13}$$

which was given in Equation (8). Therefore, the theory of Dryden and Schubauer has the restriction of isotropic turbulence entering the screen. When several screens are used, and there is sufficient space between them so they can act independently, the reduction factor applies to each screen separately. Thus, the theory of Dryden and Schubauer for the multiple screens becomes

$$fuv = \left(\frac{1}{1+K}\right)^{n/2} \tag{14}$$

where n is the number of screens.

From the above discussion, it is noted that the previous investigations considered relative values of incoming turbulence on the order of 1% and assumed isotropic turbulence. In the Compressor Research Facility, the incoming turbulence level does not follow this assumption because of the shorter decay length from the generating source and the high levels of turbulence. Consequently, due to the nonisotropic nature of the incoming turbulence and the more complicated structure of grids, honeycomb and screens, it is highly desirable to conduct detailed experiments of turbulence decay for the present conditioning system and its components.

III. EXPERIMENTAL HARDWARE

In order to conduct a valid investigation of turbulence decay on the Compressor Research Facility flow conditioning system, the Reynolds number, Mach number, incoming turbulence level and turbulence decay length had to be maintained at full-scale values. However, for practical reasons, the experiment was conducted on a 25.4 cm.diameter channel. Because the experiments were conducted on a smaller diameter channel, it is necessary to compare the boundary layer growth for the 25.4 cm. channel and the 304.8 cm. barrel of the full-scale facility (Figure 1).

Since the Compressor Research Facility's mass flow rate can vary from 6.8 to 226.8 Kg./sec., the incoming velocity in the barrel can range from 61 to 2591 cm./sec. The nondimensional inlet length,

$$L = \frac{\mu x}{a^2 U} \tag{15}$$

presented in Schlicting[9], can be used to determine the velocity profile of both the full-scale and scale devices. In Equation (15), μ is the kinematic viscosity of air, .1486 $cm.^2/sec.$ at 20°C, a is the radius of the channel, 152.4 cm. for the full-scale facility, 12.7 cm. for the small-scale channel, x is the distance into the channel and U is the velocity inlet to the channel.

Table 1 shows the values of this parameter at two locations in the full-scale facility and scale channel over the velocity range of interest.

TABLE 1

Values for L for the Full-Scale Facility and Scale Channel

X Location into Channel (cm.)	U Velocity (cm./sec.)	L for CRF Full-Scale Facility	L for Small-Scale Channel
76	61	8×10^{-6}	1.15×10^{-3}
76	2560	1.9×10^{-7}	2.74×10^{-5}
640	61	6.72×10^{-5}	9.68×10^{-3}
640	2540	1.6×10^{-6}	2.3×10^{-4}

A value for L of .001 or less indicates the velocity profile is constant over 80% of the diameter of the channel. It is indicated from the values in Table 1 that in order to maintain a constant velocity over 80% of the small-scale channel, the velocity cannot be less than 600 cm./sec. Therefore, with respect to boundary layer considerations, the investigation of this central region could be conducted on the 25.4 cm. channel over the velocity range of 600 to 2591 cm./sec.

The incoming turbulence in the Compressor Research Facility is generated by jets from the five inlet valves (Figure 1) which range in size from 35.6 to 91.0 cm. in diameter. Since it can be assumed that the geometric scale of turbulence is on the order of the valve diameters producing these jets, the incoming scale of turbulence for the full-scale facility cannot be maintained in the 25.4 cm. channel. However, since the turbulence level, Reynolds number and Mach number were maintained at the full-scale values, the scale of turbulence exiting either the full-scale or scale flow conditioners should be the same; and, therefore, the turbulence decay results of the scale experiments are applicable to the full-scale facility. In the scale experiment the initial turbulence was produced by the generator shown in Figures 3 and

4. This generator produced a pattern of turbulence similar to what would be expected in the full-scale facility while producing an incoming level of turbulence on the order of 40% at the entrance to the scale test configurations.

The experiments were conducted on the channel shown in Figures 5 and 6. The dimensions shown in Figure 5 are the hot wire traverse locations most often used when traverses in the vertical and horizontal reference planes were made. Other axial locations were obtained by rotating the center section of the channel, shown in Figure 5, 180°. The dimensions for these locations are listed in Table 3 in Section V where these locations were used. In Figure 6, the actual ports in the channel can be seen as well as the traverse mechanism installed in the vertical position midway down the channel. The inlet to the channel is shown schematically in Figure 5.

All of the configurations tested in the experiment are described in Table 2, and a picture of the various components is presented in Figure 7. Structural grids used to simulate the full-scale flow conditioner of Figure 2 are shown in detail in Figure 8. Figure 9 shows the full flow conditioner tested in the scale channel. The major difference between the full-scale hardware of Figure 2 and the test components occurs with the grids. Using a 1/2 grid on the downstream side of the three flow conditioners shown in Table 2 provided an intersection in the grid at the center of the scale channel where the turbulence measurements are of importance. In order not to significantly affect the pressure drop of these conditioners, the full-scale grid was used on the upstream side of the conditioners.

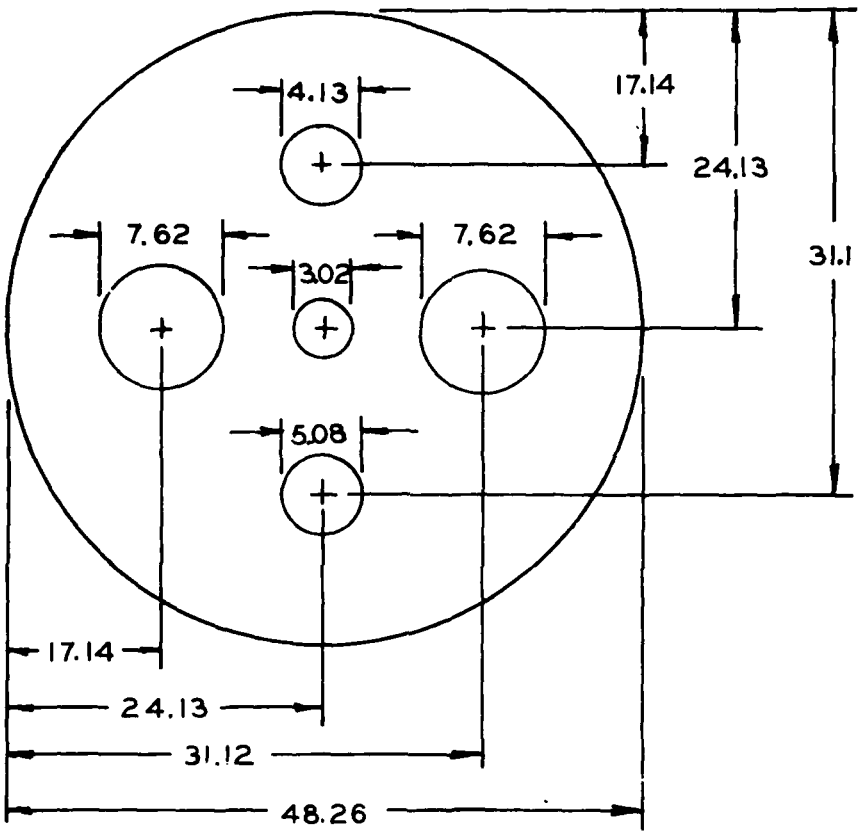

FIGURE 3 SCHEMATIC OF GENERATOR

DIMENSIONS IN CENTIMETERS

Figure 4 Turbulence generator used in experiments

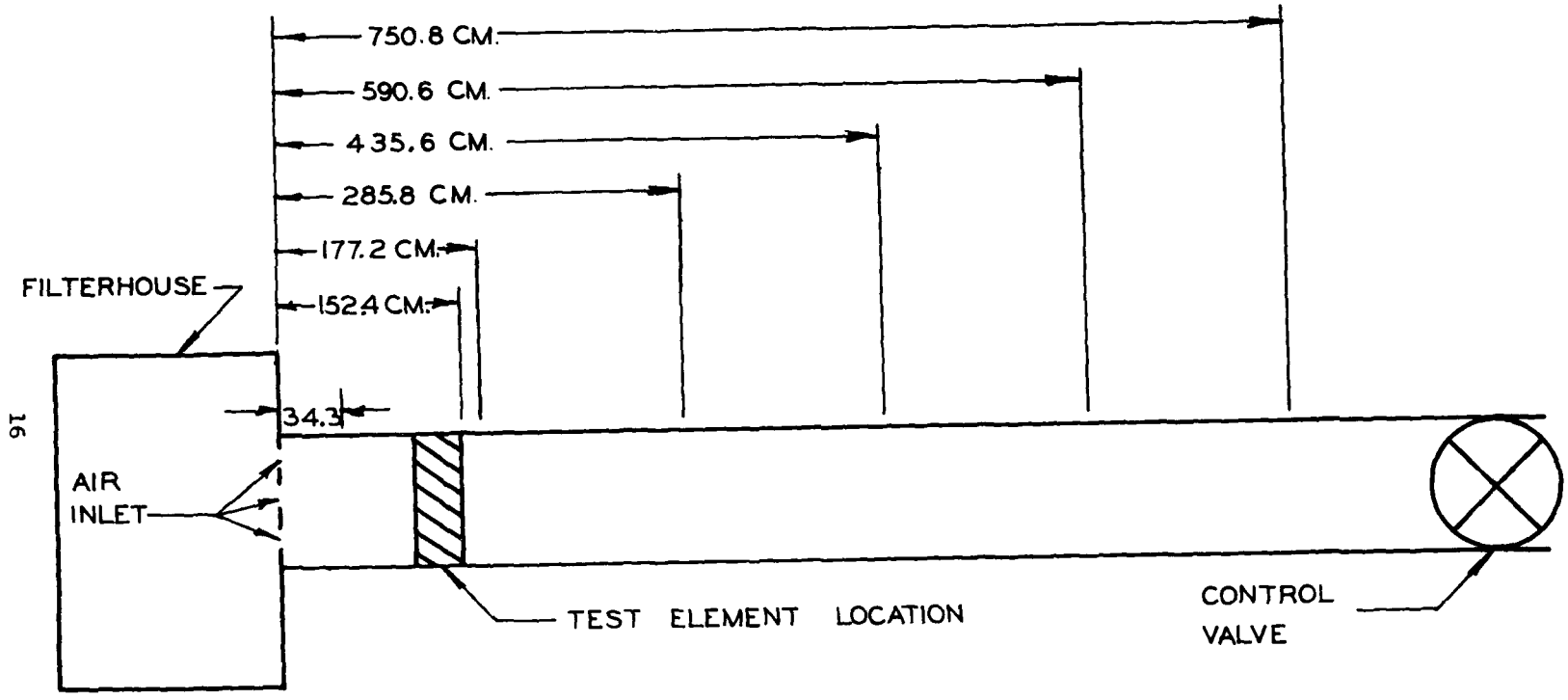

FIGURE 5 HOT WIRE TRAVERSE LOCATIONS ON THE 25.4 CM DIAMETER TEST CHANNEL

Figure 6 25.4 cm. diameter channel and the test laboratory showing traverse locations and traverse mechanism installed

TABLE 2

DESCRIPTION OF TEST CONFIGURATIONS

TEST CONFIGURATION	DESCRIPTION
Baseline	Consisted of the turbulence generator only.
Bellmouth	Consisted of a bellmouth inlet to the channel with no generator or flow conditioning element.
7.09 Mesh Screen	Consisted of a 7.09 wires/cm. screen with a wire diameter of .0432 cm. with inlet located 152.4 cm. downstream of generator.
1.18 Mesh Screen	Consisted of a 1.18 wires/cm. screen with a wire diameter of .2667 cm. with inlet located 152.4 cm. downstream of generator.
Honeycomb	Consisted of a 7.62 cm. thick honeycomb with a wall thickness of .012 cm. and a cell width of .510 cm. with inlet located at 144.78 cm. and exit at 152.4 cm. downstream of generator.
Full Grid	Consisted of a square grid, 14.60 cm. x 14.60 cm. x 11.43 cm. long. Made of .794 cm. thick material with inlet located at 140.97 cm. and exit at 152.4 cm. downstream of generator. See Figure 8.
1/2 Grid	Consisted of a square grid 7.3 cm. x 7.3 cm. x 11.43 cm. long, made of .794 cm. thick material with inlet located at 140.97 cm. and exit at 152.4 cm. downstream of generator. See Figure 8.
Perforated Plate	Consisted of a plate .0625 cm. thick with .1875 cm. diameter holes in a 60° array with a center-to-center spacing of .3125 cm. with inlet located 152.4 cm. downstream of generator.
Upstream Flow Conditioner	Consisted of a grid, 7.09 mesh screen, honeycomb, 7.09 mesh screen, 1/2 grid configuration with inlet located at 133.44 cm. and exit at 163.74 cm. downstream of generator. See Figures 2 and 7.

TABLE 2

DESCRIPTION OF TEST CONFIGURATIONS

TEST CONFIGURATION	DESCRIPTION
Downstream Flow Conditioner	Consisted of a grid, 7.09 mesh screen, honeycomb, 1.18 mesh screen, 1/2 grid configuration with inlet located at 133.44 cm. and exit at 163.74 cm. downstream of generator. See Figures 2 and 7.
Full Flow Conditioner	Consisted of the configuration shown in Figure 9 using the upstream and downstream flow conditioners with inlet located at 72.66 cm. and exit at 163.74 cm. downstream of generator. See also Figures 2 and 8.

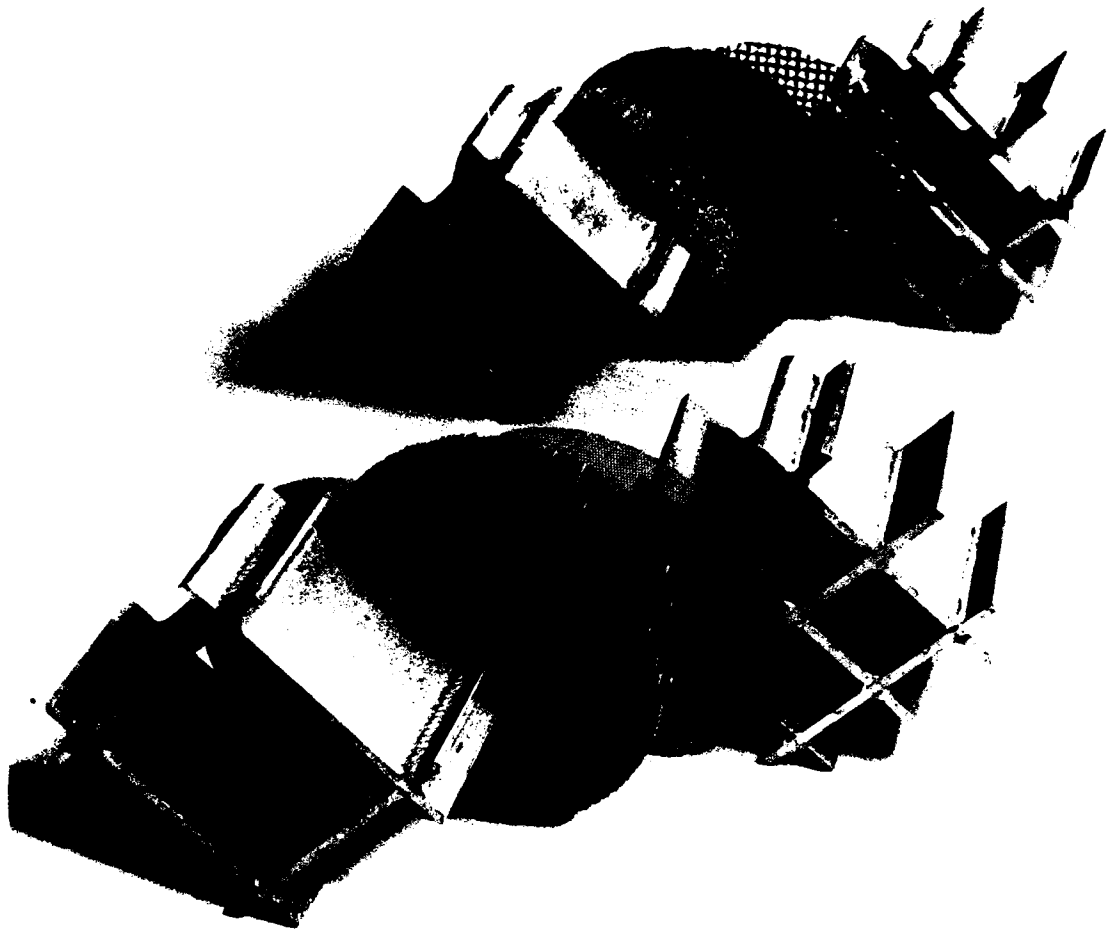

Figure 7 Relation of individual components when tested in the full flow conditioner configuration

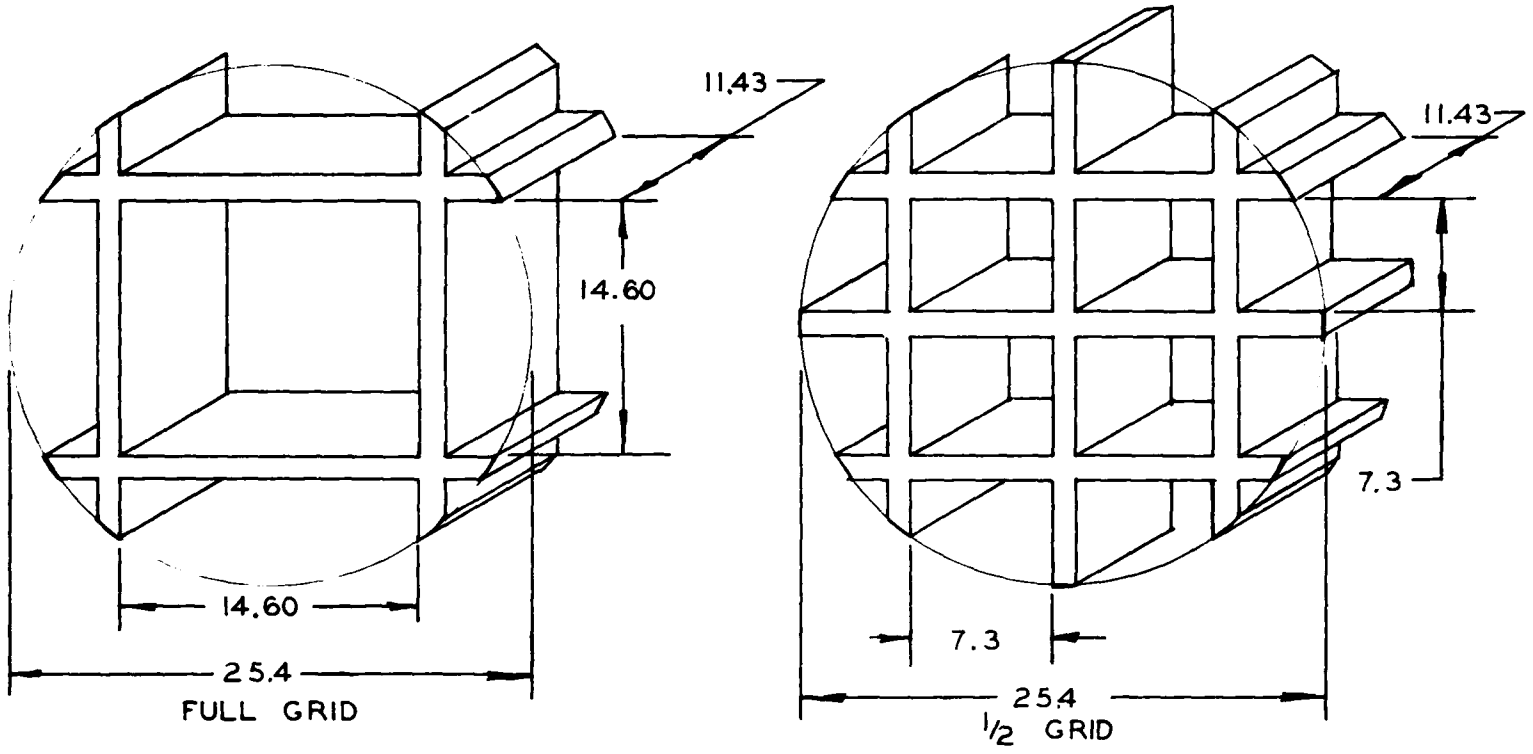

FIGURE 8 SCHEMATIC OF GRIDS
DIMENSIONS IN CENTIMETERS

Figure 9 Full flow conditioner as tested in experiment

IV. DATA ACQUISITION

Measurements were made to determine:

1. Steady-state pressures
2. Steady-state temperature
3. Time-dependent and mean velocities

Each of the above was measured using independent techniques.

A. Test Equipment

The steady-state static pressures were measured using a scanivalve which consisted of a rotary valve coupled to a single pressure transducer unit. Seven static pressures were measured down the test channel. Two known pressures, atmospheric and near vacuum, were supplied to the scanivalve to determine the calibration of the transducer during the experiments. The atmospheric pressure was measured on a standard laboratory mercury barometer while the near vacuum pressure was measured on a Wallace and Tiernan gauge.

Measurements of temperature in the test channel were made using a platinum resistance Stolab electric thermometer Model 911PL. A digital voltmeter, DYMEC model 2401C was used to read the output from the thermometer. The sensor for the thermometer was mounted near the exit of the channel in order not to disturb the flow under test conditions. Figure 10 shows the scanivalve system and temperature read-out voltmeter.

Fluctuating and mean velocities were measured using the Thermo-systems Incorporated (TSI) hot wire anemometer system also shown in Figure 10. The hot wire system consisted of a constant temperature anemometer, TSI model 1050, a power supply, TSI model 1051-2, a digital

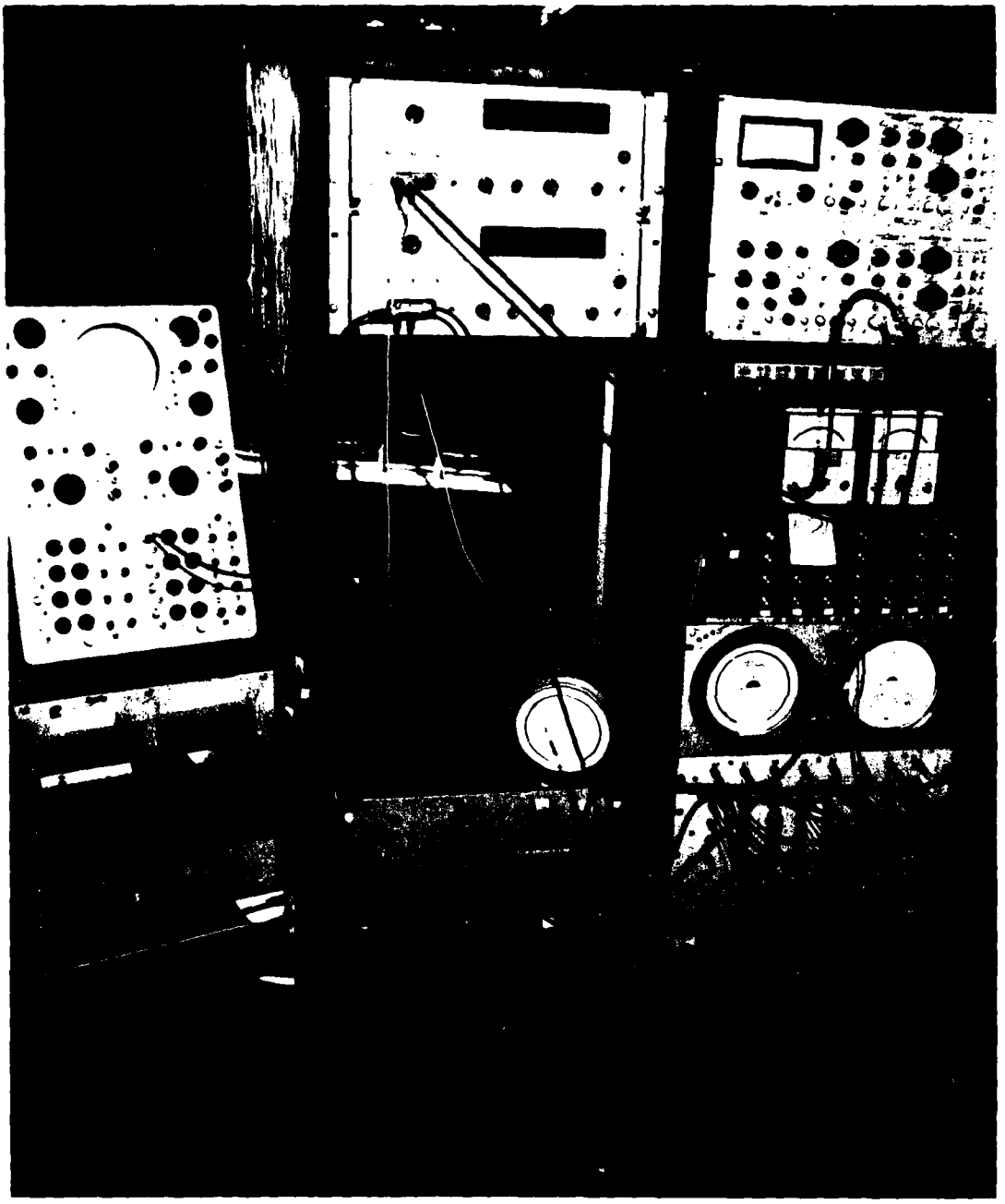

Figure 10 View of the instrumentation system used in the experiment

voltmeter, Hewlett Packard 2401C, and a root-mean-square (RMS) voltmeter, Hewlett Packard model 3400A. Since only axial velocities and turbulence levels were to be measured, a single element hot wire, TSI model 1210, was used. Calibration of the hot wire was performed on a TSI calibrator model 1125. In the velocity range of interest, this unit had a velocity measuring accuracy of ±1% when a water micromanometer was used in the setup. While calibrating a hot wire, all of the related electronic anemometer hardware was used, and a calibration of the complete system, except for the RMS voltmeter, was performed.

All of the data measured during the turbulence decay experiments were recorded with a digital computer, ModComp model II. The computer data acquisition enhanced the capability for sampling a large number of measurements and, therefore, obtaining the average value of turbulence level in the test channel.

B. Data Collection and Reduction

The hot wire data obtained from the anemometer system during the calibration and experimentation were treated in the same manner as References 4 and 10. Since the hot wire sensor responds to variations in fluid velocity, temperature and density, the temperature and density variations between calibration and experimentation must be determined. Using Nusselt number, Nu, and Reynolds number, Re, the temperature and density variations can be reconciled by the following relationship:

$$Nu \left(\frac{Tf}{Tm}\right)^{.17} = A + B\ Re^{m} \qquad (16)$$

and

$$Nu = \frac{H_{f/\ell w}}{\pi K_f (Tw-Tf)} \quad , \tag{17}$$

where A, B and m are arbitrary constants, H_f is the heat transfer rate, K_f is the thermal conductivity at Tm, ℓw is the wire length and Tw and Tf are the static temperature of the wire and fluid respectively. The mean temperature, Tm, is the average temperature between the wire and the fluid, given by Tm = 1/2 (Tf + Tw). The Reynolds number used in Equation (16) is

$$Re = \frac{U_f dw}{\mu_f} \tag{18}$$

where μ_f is the kinematic viscosity of the fluid evaluated at Tm and the static pressure of the fluid.

For the low wire Reynolds numbers of this experiment it has been suggested[4] that the constant m in Equation (16) be equal to .45. Using the above procedure, a calibration curve for one of the wires used during the experimentation is shown in Figure 11.

As stated in Reference 4, Equation (16) is restricted to forced convection conditions and is only valid when

$$Re > 2Gr^{1/3} \tag{19}$$

where Gr is the Grashof number which is defined as

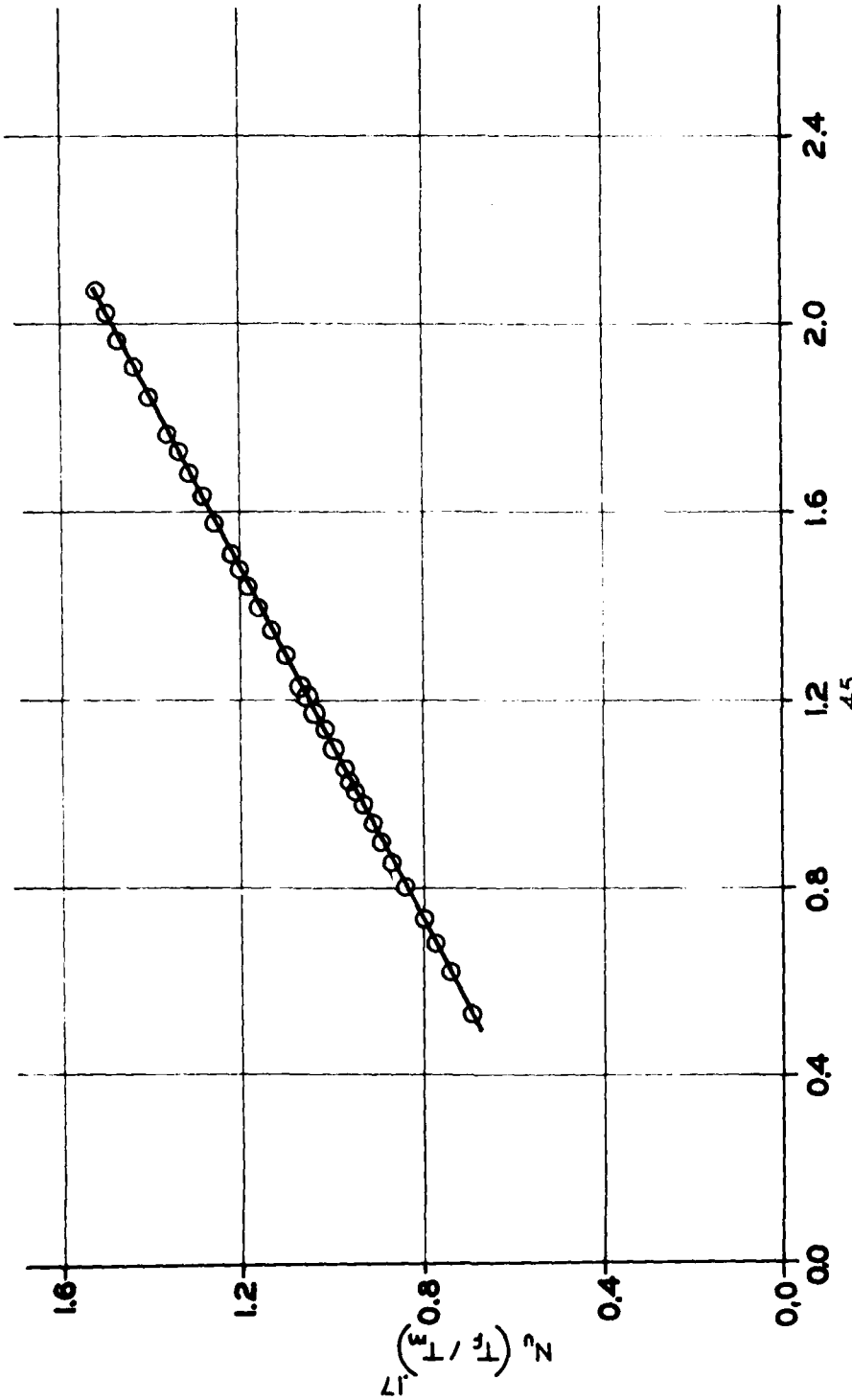

FIGURE 11 CALIBRATION CURVE FOR PROBE 8479.

$$Gr = \frac{dw^3 (Tw-Tf)}{(\mu_f)^2 \, Tf} \tag{20}$$

This condition was always satisfied during this experimentation.

The calibration relationships can also be extended to the fluctuating component of the flow and

$$\tau = \frac{2 \, Nu \left(\frac{Tf}{Tm}\right)^{.17} \frac{e^1}{E}}{.45 \, B(Re)^{.45}} \tag{21}$$

Equation (21) is restricted to

$$\frac{Nu \left(\frac{Tf}{Tm}\right)^{.17} \frac{e^1}{E}}{Nu \left(\frac{Tf}{Tm}\right)^{.17} - A} << 1 \tag{22}$$

which was satisfied in the experiment even for the high turbulence levels.

Because the turbulence level entering the channel was on the order of 40%, possible heat transfer and non-linear effects of the hot wire must be considered. Sandborn[11] shows that, when the scale of turbulence is very small or very large compared with the hot wire diameter, the effect of turbulence level on heat transfer is relatively small regardless of intensity of turbulence. For example, with a turbulence level of 12% and a ratio of the scale of turbulence to the diameter of the hot wire of 10, a 10% increase in heat transfer would result. Therefore, since it is estimated that for this experiment,

this ratio is greater than 100, heat transfer effects should be less than 10% at the turbulence level of 40% and even less at lower turbulence levels.

Because the lowest mean velocity is greater than 600 cm./sec., there should be minimal non-linear effects of the hot wire. Rivir[10] estimated that at a mean velocity of 150 cm./sec., a turbulence level of 60% would cause an error of 7% in the mean value of velocity. Since this experiment is conducted at four times the mean velocity of 150 cm./sec., this error should be greatly reduced. Therefore, a non-linear correction to the mean velocity was not considered necessary for this experiment.

Velocity calibration of the hot wire was carried out in the above manner which, as previously indicated, calibrated the anemometer system. The remaining elements of calibration interest are the RMS voltmeter and the computer.

A calibration check of the RMS voltmeter was performed in the test setup. A signal generator was applied to the input of the RMS voltmeter and to an oscilloscope. The output on both the oscilloscope and the RMS voltmeter was observed to indicate the same RMS values.

Since the hot wire RMS and DC voltage and the temperature were recorded on the computer, the interactions of the various meters with one another and with the computer were investigated. It was found that the hot wire DC voltage meter (Hewlett Packard model 2401C) introduced some AC noise picked up by the RMS voltmeter which would

indicate approximately a 10% higher turbulence level. This interaction was eliminated when the system was completely interfaced with the computer. Apparently, the computer grounding system alleviated the problem. A calibration check was performed on the computer by observing no difference between meter read-out and computer print-out.

The scanivalve data were also recorded by the computer. No calibration checks of this sytem were considered necessary because the computer calibrated the scanivalve transducer during the experiment, using the two known pressures of the atmosphere and the near vacuum reference.

It was found that the RMS voltmeter would not accurately record the low voltages observed in the center of the flow while concurrently being set up to read the higher values of voltage found at the walls. Because of this high dynamic range of turbulence across the channel, a traverse of the center 11.34 cm. was used throughout this experiment.

To obtain one turbulence level data point across the test channel, the computer would sample and record 63 points as the hot wire was traversed across the center 11.43 cm. A traverse was made in both the vertical and horizontal planes, and a total of 126 data points per location was obtained. An average of the 126 readings would then be used to indicate the turbulence level of a particular station in the channel. The traverse mechanism with a hot wire installed is shown in Figure 12.

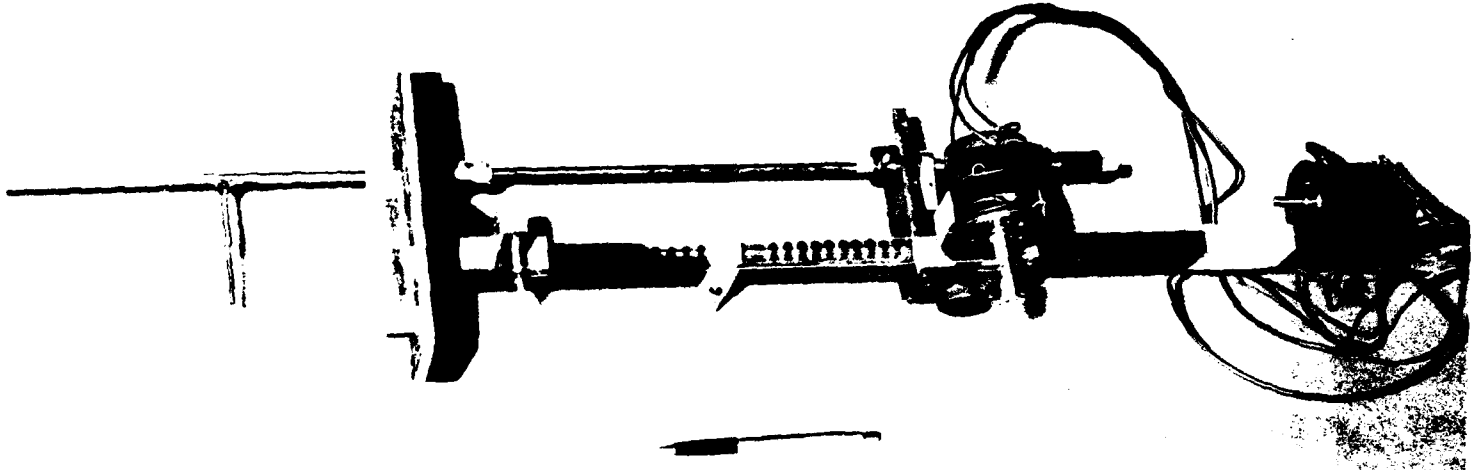

Figure 12 Traverse mechanism with a hot wire installed

V. EXPERIMENTAL RESULTS

In order to determine if low turbulence levels could be measured with the experimental hardware, a bellmouth was installed on the channel inlet (see Table 2). It was felt that this configuration would produce the minimum turbulence level profile down the channel while exhibiting an inlet turbulence level of less than 1%. At first, relatively high values of turbulence were obtained. In an attempt to correct this high turbulence condition, a 91 cm. cubic filterhouse was installed (see Figure 4). Although the filterhouse reduced the turbulence level, it was also necessary to seal the cracks in the doors of the laboratory near the inlet to the channel before a turbulence level of less than 1% was obtained at the inlet to the channel. Apparently, colder outside air leaking into the laboratory while the experiment was in progress caused significant temperature fluctuations within the channel, and these fluctuations were observed as higher turbulence levels.

The velocity and turbulence level profiles for the bellmouth configuration are shown in Figures 13 and 14. At 750 cm. downstream from the bellmouth throat, the turbulence level is significantly affected by the walls of the channel as noted in the profile. For comparison, the velocity and turbulence level profiles for the full flow conditioner (Table 2) are shown in Figures 15 and 16. The velocity and turbulence levels are both affected by the grid in the center of the channel. At 587 cm. downstream from the exit of the conditioner, the turbulence level is less affected by the wall than in the bellmouth

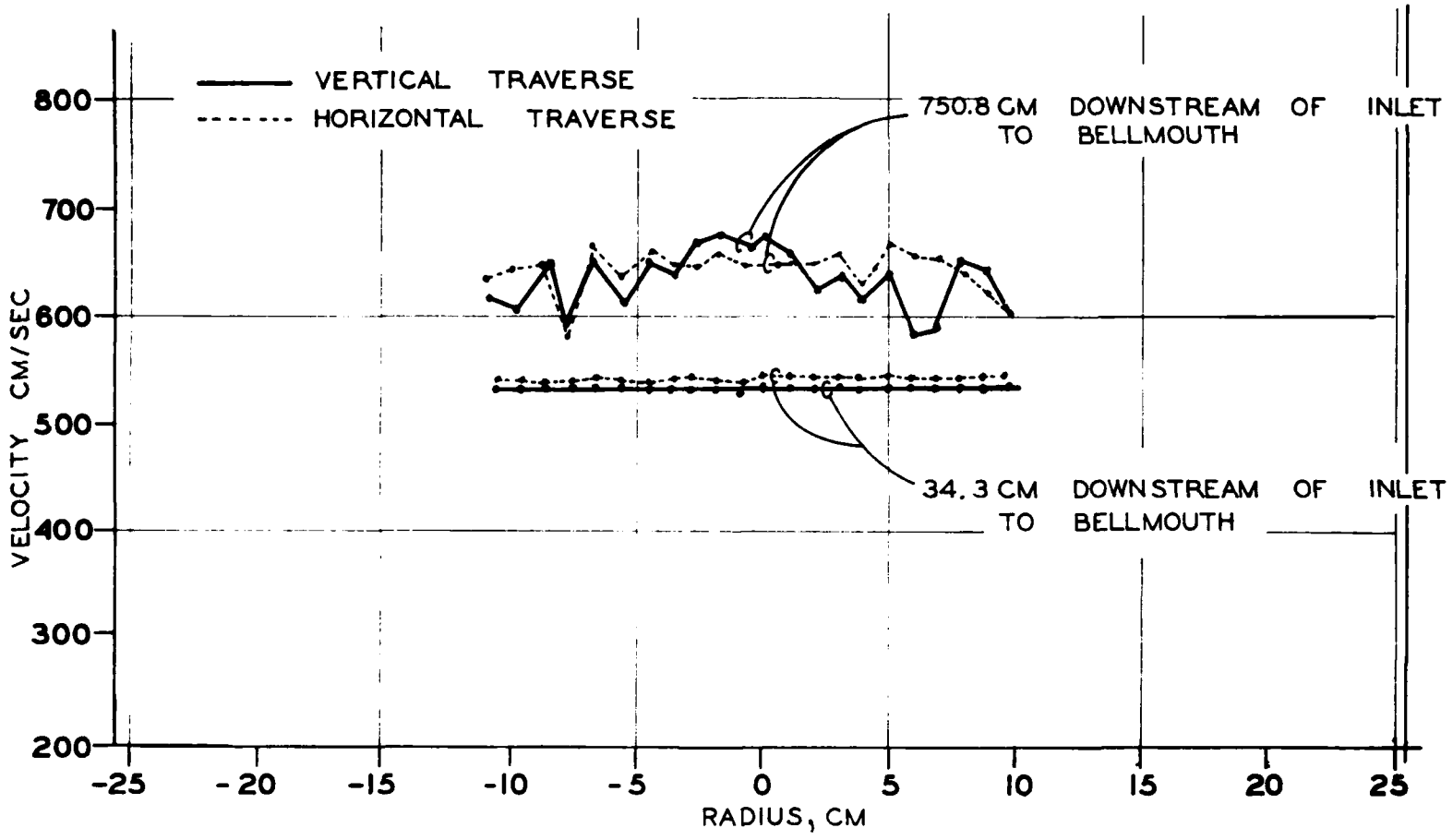

FIGURE 13 VELOCITY PROFILE DATA FOR BELLMOUTH AT 34.3 CM AND 750.8 CM DOWNSTREAM FROM BELLMOUTH INLET

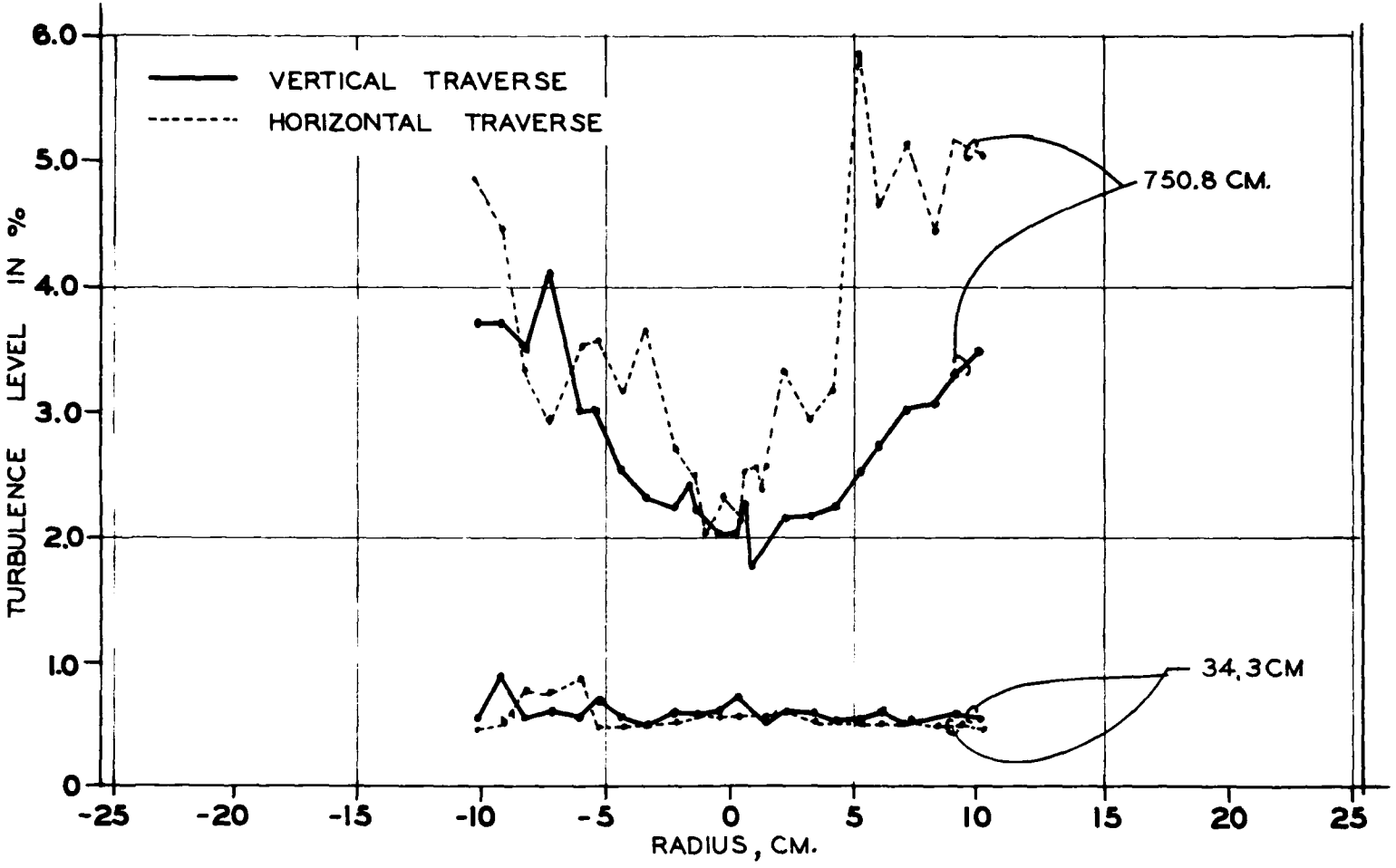

FIGURE 14 TURBULENCE PROFILE DATA FOR BELLMOUTH AT 34.3 CM. AND 750.8 CM. DOWNSTREAM FROM BELLMOUTH INLET.

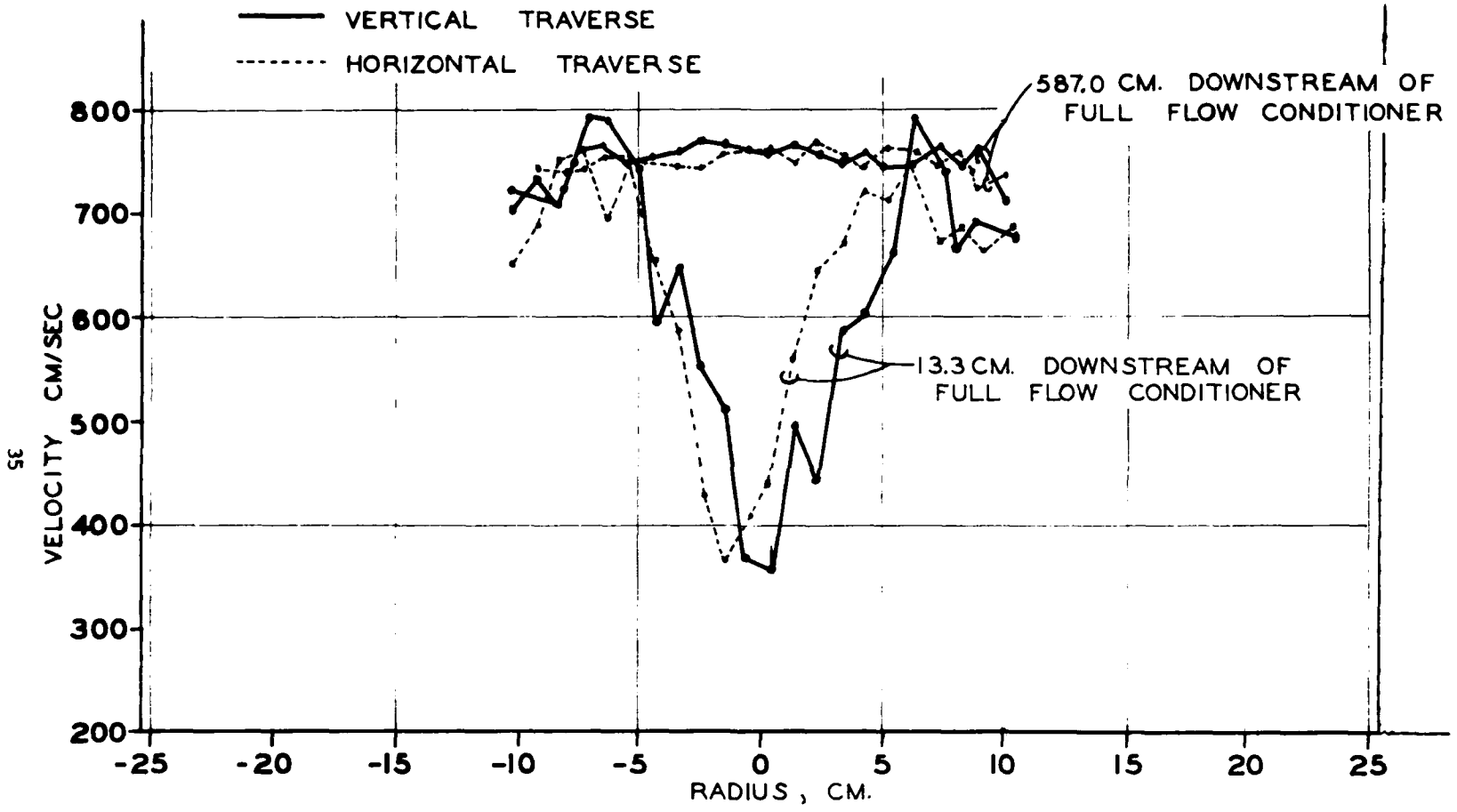

FIGURE 15 VELOCITY PROFILE DATA FOR FULL FLOW CONDITIONER AT 13.3 CM. AND 587.0 CM. FROM CONDITIONER EXIT.

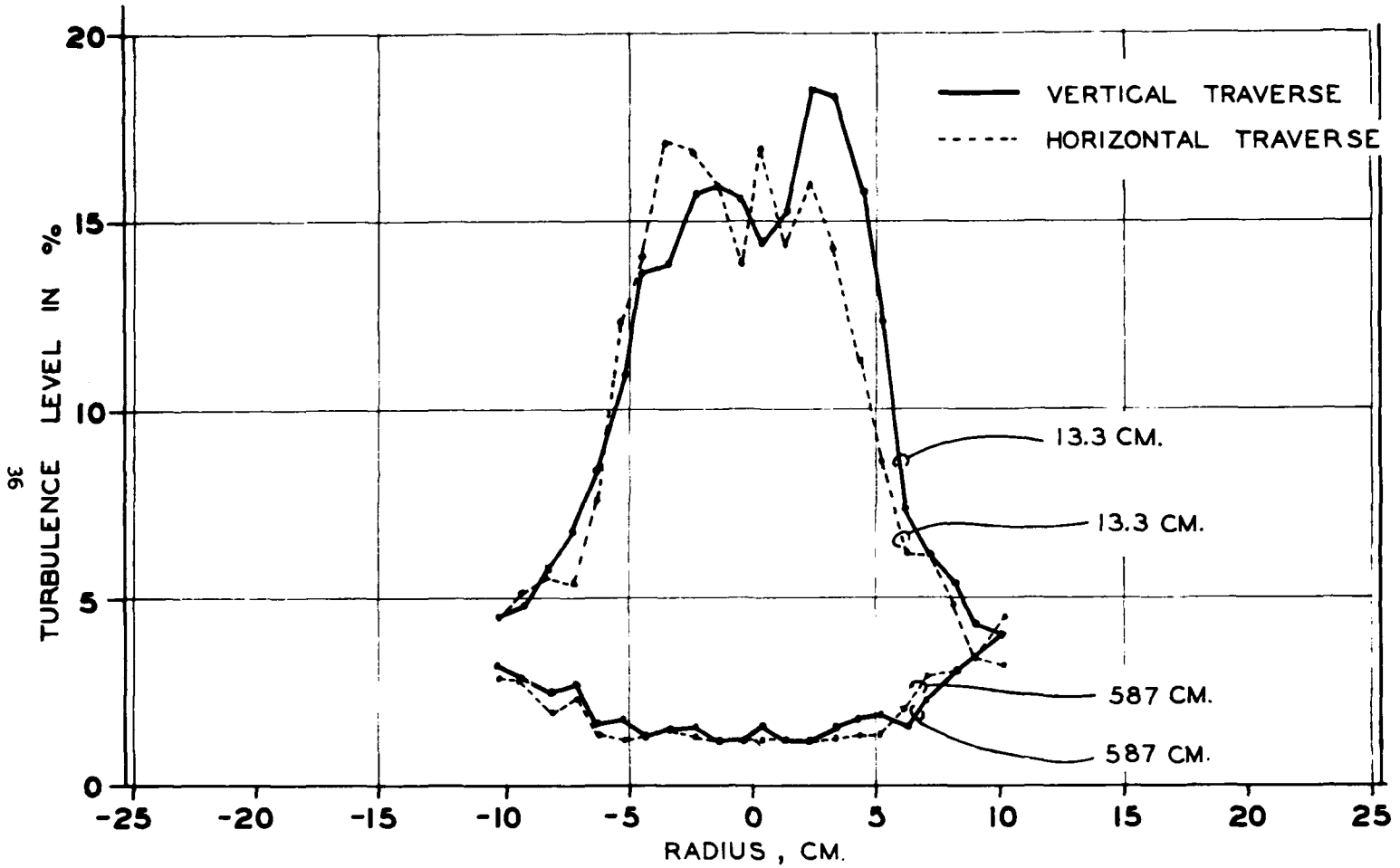

FIGURE 16 TURBULENCE PROFILE DATA FOR FULL FLOW CONDITIONER AT 13.3 CM. AND 587 CM. FROM CONDITIONER ENTRANCE

configuration. It is felt that the boundary layer is being energized by the full flow conditioner and, therefore, is thinner at the downstream location than for the bellmouth configuration.

Because of the effect of the walls on the profiles of turbulence and velocity, an averaging technique across the complete traverse would be misleading at the downstream locations of the channel, and also where the profile is significantly affected by the grid of a flow conditioner near the inlet to the channel, an average near the centerline would be misleading. Therefore, it was decided that an average across the traverse would be used at the two locations nearest the inlet to the channel while a centerline average of ten points (five points each from the horizontal and vertical traverses) would be used for the remaining four downstream locations.

All of the configurations listed in Table 2 except the full grid were tested for turbulence decay, and the data are presented in Table 3. From Table 3 it is observed that the average velocity in the channel generally increases down the channel. This increase in velocity is the result of the boundary layer thickness increasing down a channel with constant mass flow. It is noted that the velocity recorded at 34.3 cm. downstream from the channel inlet for all test configurations, except the bellmouth, is exceedingly high. This high velocity is a result of the jet produced by the center hole in the generator (see Figure 3). The inlet turbulence level measured at this location determined the consistency between test configurations.

TABLE 3

AVERAGE LEVELS OF VELOCITY AND TURBULENCE LEVEL AT SEVERAL DOWNSTREAM POSITIONS FOR VARIOUS TEST CONFIGURATIONS

CONFIGURATION / DOWN-STREAM DISTANCE	BELLMOUTH		BELLMOUTH	
CENTIMETERS	$U\frac{cm}{sec}$	τ	$U\frac{cm}{sec}$	τ
34.3	534.	.59	1441.	.913
153.9	555.	.97	1494.	1.36
306.3	594.	1.30	1571.	1.37
458.7	616.	1.40	1631.	1.17
575.6	630.	1.80	1305.	1.37
750.8	633.	2.24	1308.	2.28

TABLE 3 (Cont'd)

AVERAGE VALUES OF VELOCITY AND TURBULENCE LEVEL AT
SEVERAL DOWNSTREAM POSITIONS FOR VARIOUS TEST CONFIGURATIONS

CONFIGURATION / DOWN-STREAM DISTANCE	BASELINE		7.09 MESH SCREEN		1.18 MESH SCREEN		HONEYCOMB	
CENTIMETERS	$U\frac{cm}{sec}$	τ	$U\frac{cm}{sec}$	τ	$U\frac{cm}{sec}$	τ	$U\frac{cm}{sec}$	τ
34.3	1865.	40.80	1603.	42.8	1695.	42.00	1682.	41.10
177.2	762.	15.40	582.	6.10	610.	7.14	619.	7.97
285.8	753.	7.70	628.	4.40	649.	4.54	695.	5.43
435.6	774.	5.00	658.	2.90	674.	3.64	713.	3.90
590.6	805.	3.80	664.	2.40	671.	2.92	765.	2.90
750.8	811.	3.70	680.	2.60	674.	3.20	811.	2.70

TABLE 3 (Cont'd)

AVERAGE VALUES OF VELOCITY AND TURBULENCE LEVEL AT
SEVERAL DOWNSTREAM POSITIONS FOR VARIOUS TEST CONFIGURATIONS

CONFIGURATION / DOWN-STREAM DISTANCE	BASELINE		7.09 MESH SCREEN		1.18 MESH SCREEN		HONEYCOMB	
CENTIMETERS	$U\frac{cm}{sec}$	τ	$U\frac{cm}{sec}$	τ	$U\frac{cm}{sec}$	τ	$U\frac{cm}{sec}$	τ
34.3	344.1	41.30	3380.	41.80	3475.	41.30	3682.	40.90
177.2	1417.	16.10	1283.	6.47	1271.	7.14	1478.	8.48
285.8	1494.	8.65	1372.	4.40	1342.	5.05	1554.	5.82
435.6	1506	5.18	1451.	3.10	1402.	3.49	1646.	4.22
590.6	1533.	3.86	1518.	2.54	1426.	2.99	1673.	3.11
750.8	1530.	3.38	1509.	2.52	1469.	3.12	1679.	3.00

TABLE 3 (Cont'd)

AVERAGE VALUES OF VELOCITY AND TURBULENCE LEVEL AT
SEVERAL DOWNSTREAM POSITIONS FOR VARIOUS TEST CONFIGURATIONS

CONFIGURATION / DOWN-STREAM DISTANCE	1/2 GRID		PERFORATED PLATE		UPSTREAM FLOW CONDITIONER		DOWNSTREAM FLOW CONDITIONER		FULL FLOW CONDITIONER	
CENTIMETERS	U $\frac{cm}{sec}$	τ	U $\frac{cm}{sec}$	τ	U $\frac{cm}{sec}$	τ	U $\frac{cm}{sec}$	τ	U $\frac{cm}{sec}$	τ
34.3	2115.	38.40	1783.	41.10	-	-	1664.	42.20	1600.	41.20
177.2	796.	14.20	614.	11.00	722.	5.60	652.	8.78	689.	8.20
285.8	786.	5.36	671.	6.49	763.	2.62	634.	3.40	677.	2.92
435.6	822.	3.67	719.	3.89	799.	1.99	668.	2.07	704.	1.66
590.6	838.	3.13	750.	3.30	814.	1.65	699.	1.57	731.	1.26
750.8	860.	2.80	763.	3.12	-	-	700.	1.62	747.	1.22

TABLE 3 (Cont'd)

AVERAGE VALUES OF VELOCITY AND TURBULENCE LEVEL AT
SEVERAL DOWNSTREAM POSITIONS FOR VARIOUS TEST CONFIGURATIONS

CONFIGURATION / DOWN-STREAM DISTANCE	1/2 GRID		PERFORATED PLATE		UPSTREAM FLOW CONDITIONER		DOWNSTREAM FLOW CONDITIONER		FULL FLOW CONDITIONER	
CENTIMETERS	$U\frac{cm}{sec}$	τ	$U\frac{cm}{sec}$	τ	$U\frac{cm}{sec}$	τ	$U\frac{cm}{sec}$	τ	$U\frac{cm}{sec}$	τ
34.3	3493.	41.40	3414.	41.20	3499.	42.00	3206.	41.30	2829.	42.70
177.2	1487.	14.70	1283.	13.40	1384.	5.52	1334.	8.01	1268.	7.46
285.8	1521.	5.70	1436.	7.72	1445.	2.60	1308.	3.02	1256.0	2.65
435.6	1548.	3.68	1507.	4.50	1503.	2.14	1481.	2.00	1314.0	1.66
590.6	1603.	3.02	1551.	3.60	1555.	1.71	1526.	1.59	1369.	1.33
750.8	1609.	3.05	1564.	3.34	1597.	1.59	1631.	1.49	1402.	1.30

A comparison of the turbulence decay for the bellmouth and baseline configurations is shown in Figure 17 for 700 cm./sec. and Figure 18 for 1340 cm./sec. It can be seen in both figures that the centerline turbulence level increases down the channel for the bellmouth case. Corrsin[12] has indicated that the wall's effect on the centerline turbulence could be significant when investigating the final period of decay. The wall's effect was not investigated further in this experiment; however, the bellmouth tests provide a minimum turbulence level for the experiment.

The baseline shown on both Figures 17 and 18 shows the untreated turbulence decay and forms a basis for applying any of the turbulence reduction theories presented earlier. It should be noted that the turbulence for the baseline configuration cannot be considered isotropic. The baseline decay curve shows only initial period of decay characteristics. As shown in the figures, there is a difference in entrance turbulence level between the full-flow conditioner and both downstream and upstream conditioners. The inlet location to the test compressor in the full-scale facility is shown in these figures in relation to the exit plane of the flow conditioner configurations tested.

A comparison of Figures 17 and 18 shows that the turbulence decay for the baseline behaves the same for both velocities. This similarity would be expected because the mechanism for producing the turbulence has not changed. The lower velocity of 700 cm./sec. is above the value of velocity required for shedding of eddies, and the flow has not become sonic in the generator at the higher velocity of 1340 cm./sec.

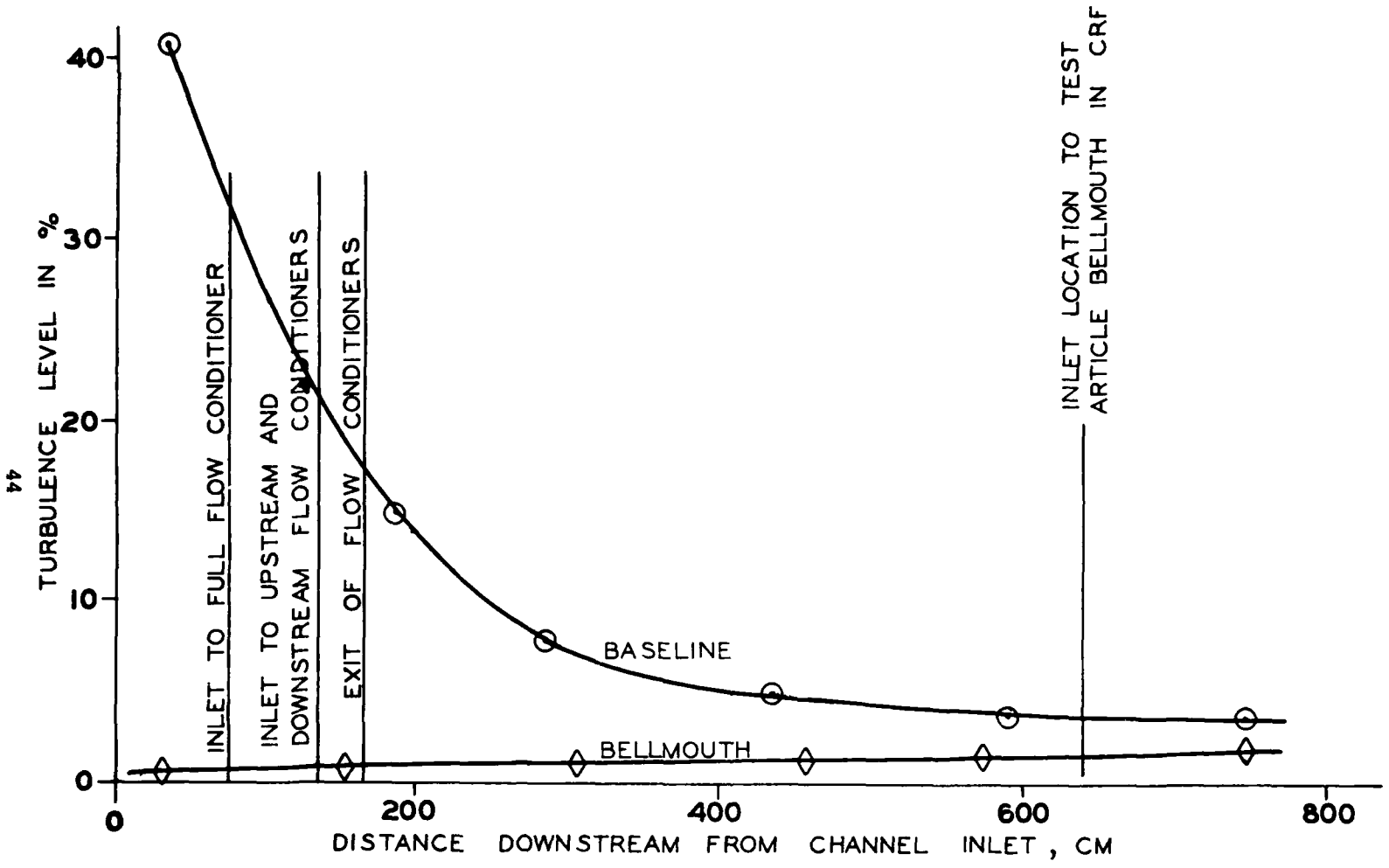

FIGURE 17 TURBULENCE DECAY DATA FOR BASELINE AND BELLMOUTH CONFIGURATION AT 700 CM/SEC., SHOWING SIMULATED CRF DECAY LENGTH

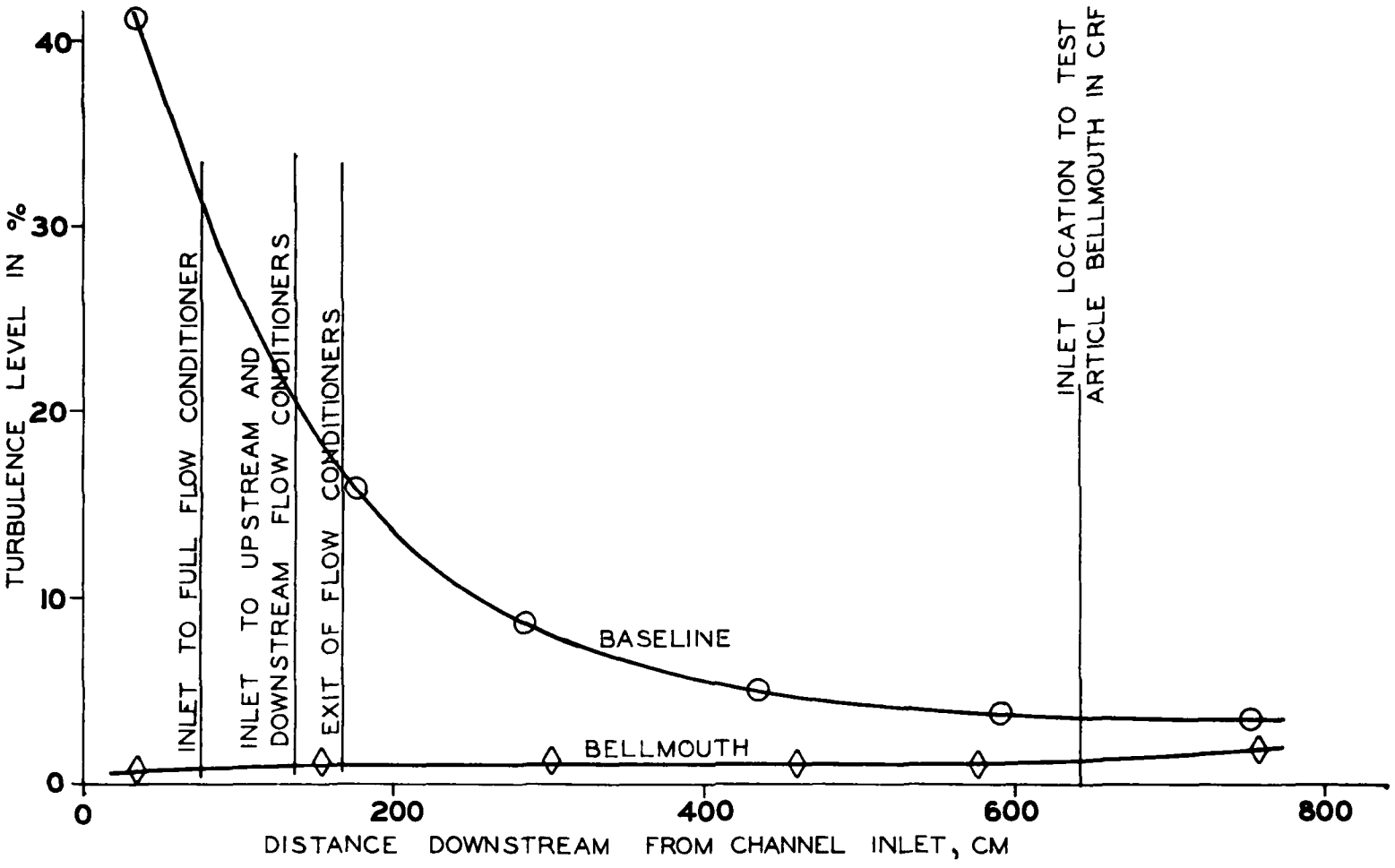

FIGURE 18 TURBULENCE DECAY DATA FOR BASELINE AND BELLMOUTH CONFIGURATION AT 1340 CM/SEC., SHOWING SIMULATED CRF DECAY LENGTH.

In order to compare the turbulence reduction across a conditioning element to the theories presented earlier, the pressure drop of the test configurations must be measured. The pressure drop was measured with a water micromanometer while the configuration was installed in the test channel. Figures 19a and 19b present the pressure drop data for the test configurations over the range of velocity of interest for the Compressor Research Facility. Figure 20 shows the turbulence reduction factors measured directly downstream of the flow conditioning element at 700 and 1340 cm./sec. as a function of the test configuration pressure drop coefficient. The theoretical reduction factors given by Equation (8) are represented by the curve in the figure.

In order to eliminate the contiguous effect of the screen, Reference 8 computed a reduction factor for a screen using a decay theory and data obtained further downstream. By applying the initial period of decay law Equation (2), a value of turbulence level directly behind the test configuration can be projected from the data obtained at 133.4 cm. downstream of the conditioning element exit. Figure 21 shows the turbulence reduction values obtained in this manner as a function of the pressure drop coefficient. It is observed from Figure 21 that this method of computing the turbulence reduction factor improves the correlation to the theory for the data of individual elements. However, there is no improvement for the three flow conditioning systems. One possibility for this result may be in the way the pressure drop was measured for the test configurations. For the three flow conditioning systems, the downstream pressure reading may be in error due to the velocity profile directly behind the system (see Figure 15) where the pressure

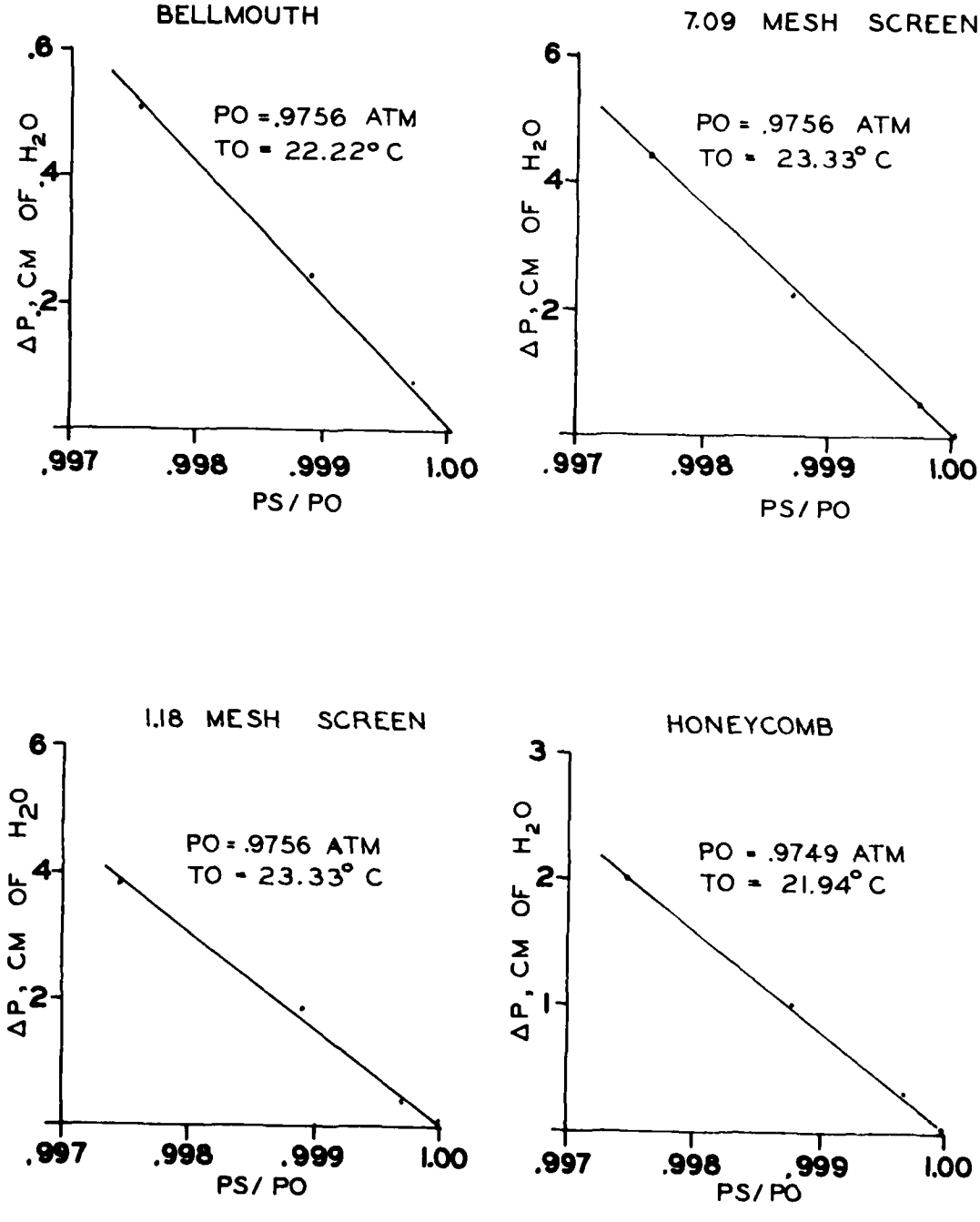

FIGURE 19a TEST CONFIGURATION PRESSURE DROP AS A FUNCTION OF UPSTREAM PS/PO

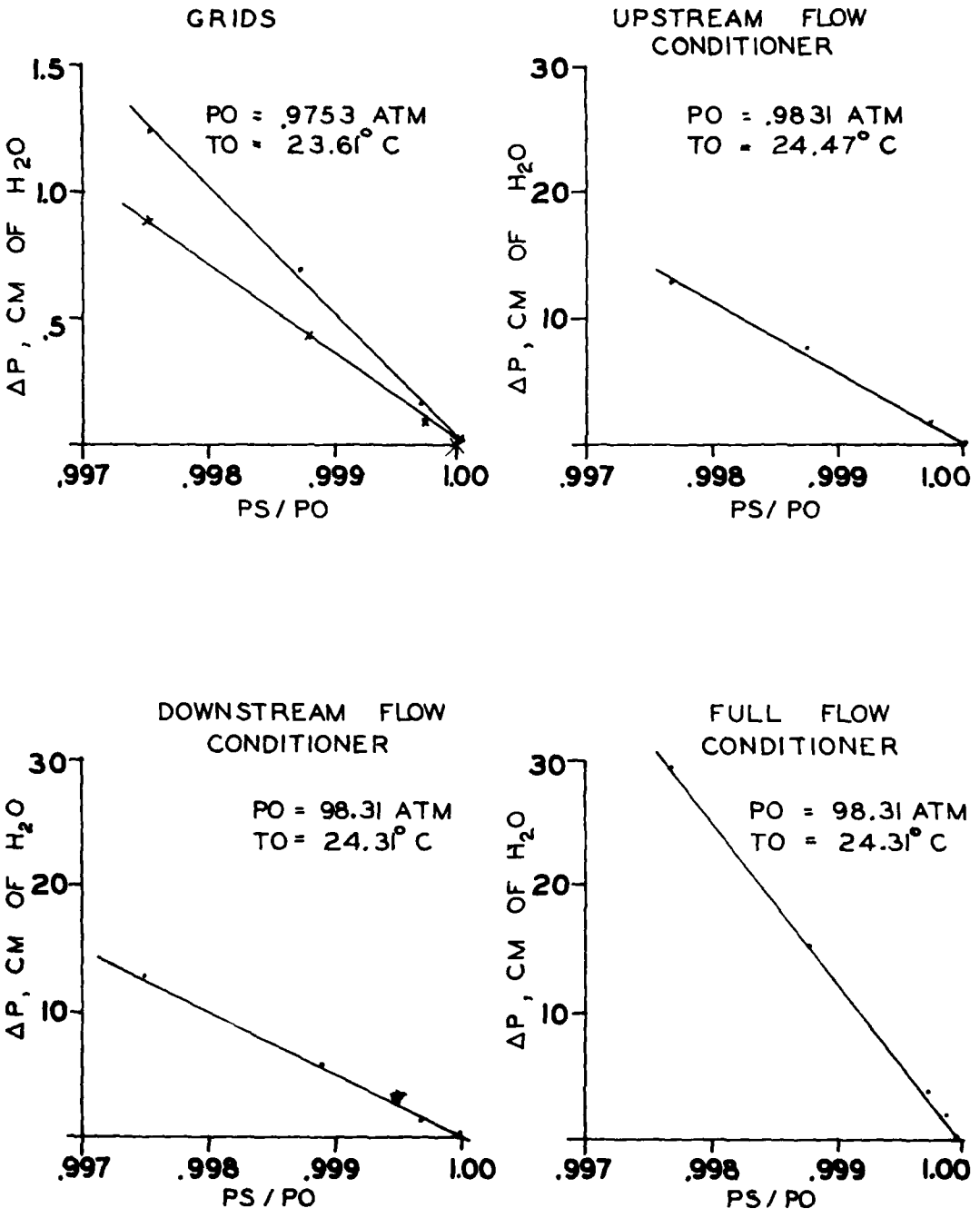

FIGURE 19b TEST CONFIGURATION PRESSURE DROP AS A FUNCTION OF UPSTREAM PS/PO

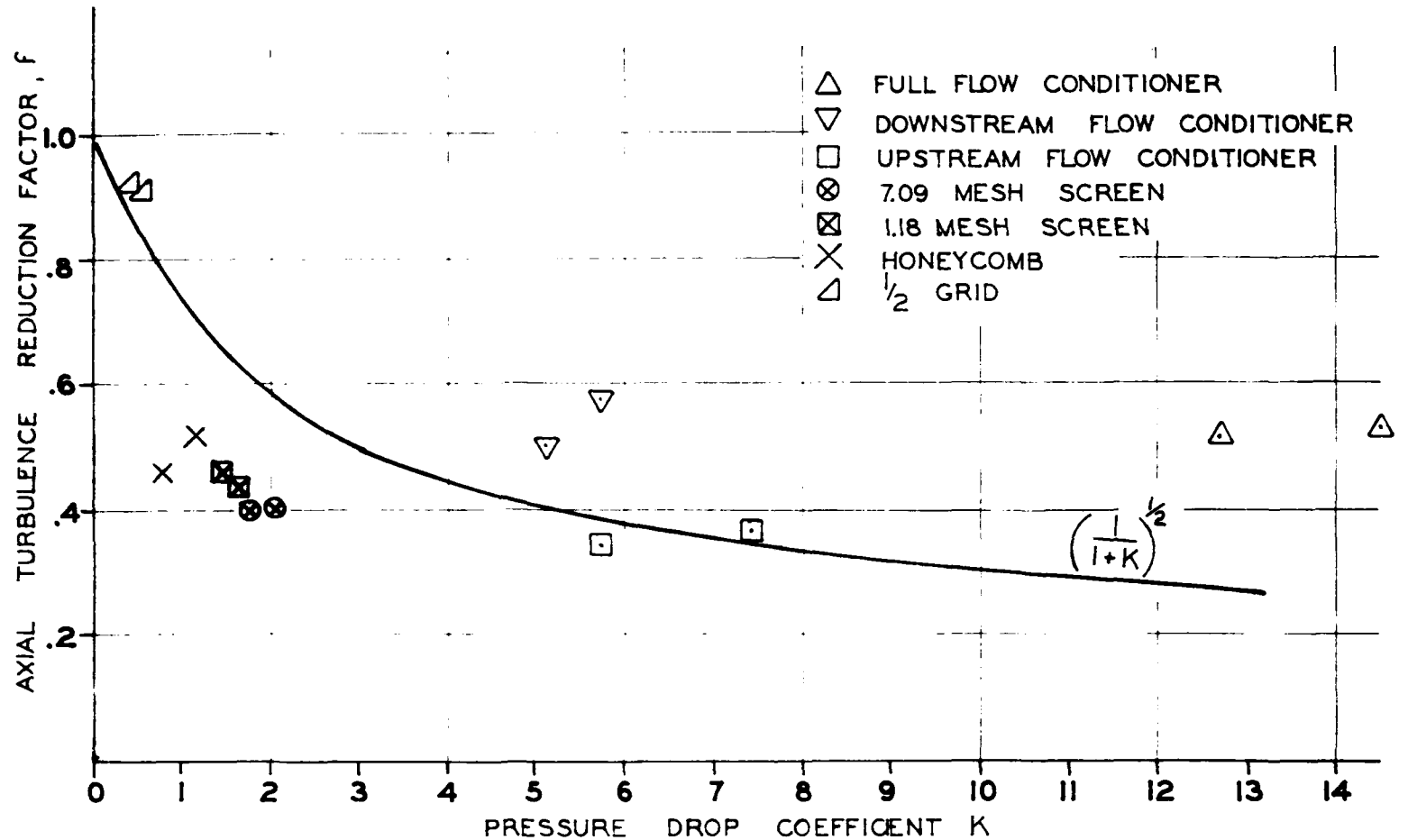

FIGURE 20 TEST CONFIGURATION PRESSURE DROP COEFFICIENTS AS A FUNCTION OF REDUCTION FACTOR MEASURED DIRECTLY DOWNSTREAM OF TEST CONFIGURATION

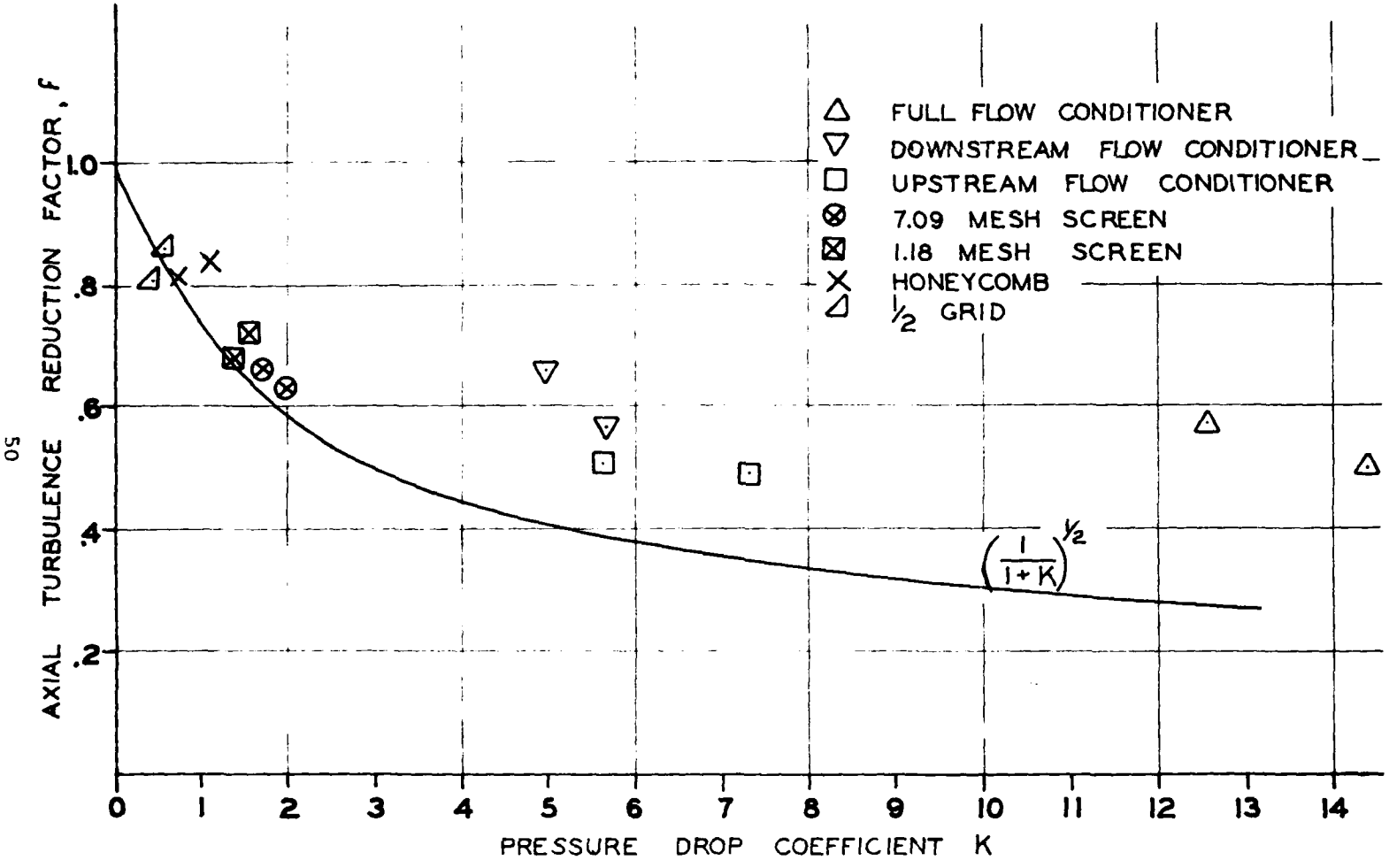

FIGURE 21 TEST CONFIGURATION PRESSURE DROP COEFFICIENT AS A FUNCTION OF REDUCTION FACTOR AS COMPUTED IN REFERENCE 8

measurement was made. However, to result in a better correlation, the measurement of the pressure drop across the flow conditioning element must be 300% too high. Therefore, it is believed that the three flow conditioning systems do not behave as Dryden and Schubauer would predict.

Turbulence decay for the 7.09 and 1.18 mesh screens is presented in Figure 22 for 700 cm./sec. and Figure 23 for 1340 cm./sec. The curves in the figures are the result of applying the initial decay theory, Equation (2), to the 7.09 mesh screen at 133.4 cm. downstream of the screen. Close agreement with the data beyond 130 cm. is observed. Except for the turbulence level at the first position downstream from the screen, the actual decay behind the screen behaves similarly to the baseline decay. Also, if an attempt were made to apply the final period of decay, Equation (3), to the data, a correlation would not be observed. Therefore, it is suggested that at these high levels of turbulence, both viscous and inertia forces are of importance, and the turbulence will not decay as the final period of decay equation would predict until much further downstream where turbulence levels would be below 1%. Thus, to obtain final period of decay characteristics, the turbulence must decay to less than 1% and become isotropic as Corrsin[11] has suggested.

Again, as in Figures 17 and 18, the data at 700 and 1340 cm./sec. are similar, and as before, the turbulence producing mechanisms of the generator and the screen are the same for both velocities.

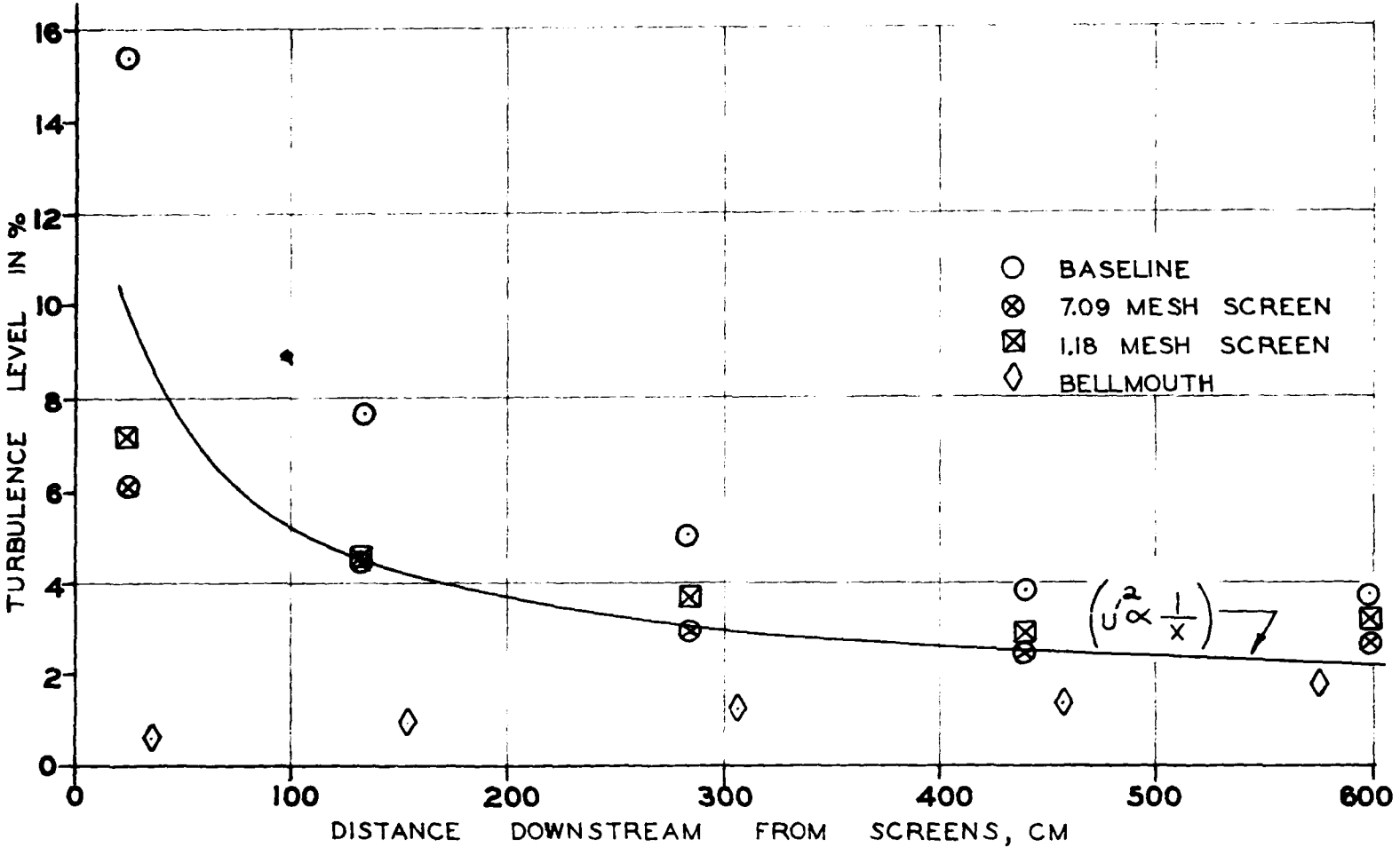

FIGURE 22 TURBULENCE DECAY DATA FOR SCREENS AT 700 CM/SEC

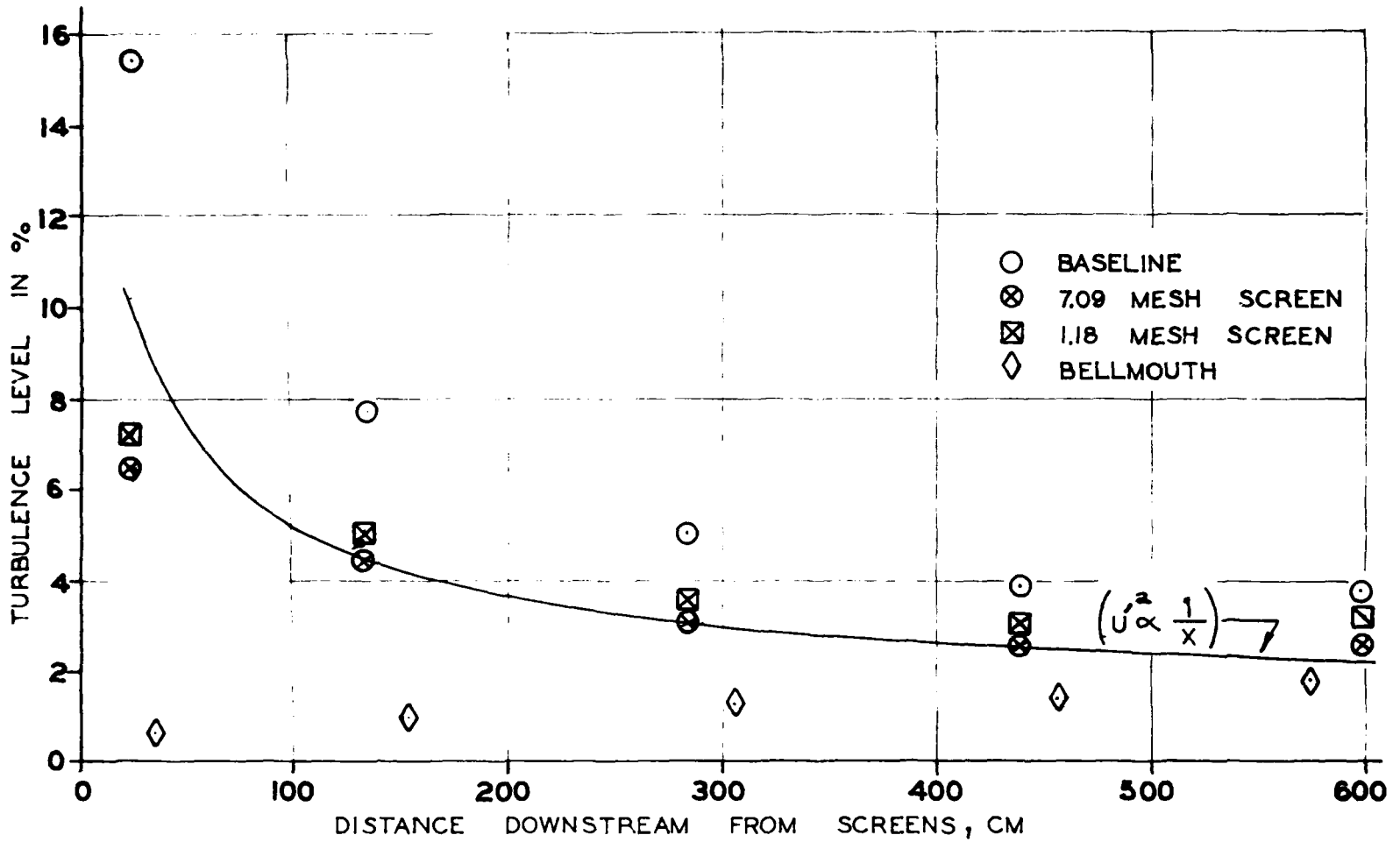

FIGURE 23 TURBULENCE DECAY DATA FOR SCREENS AT 1340 CM/SEC

Turbulence decay for the three flow conditioners listed in Table 2 is shown in Figure 24 for 700 cm./sec. and Figure 25 for 1340 cm./sec. The curve in these figures is the result of applying the initial period of decay equation as above to the full-flow conditioner data. In these figures, the first downstream location shows close agreement with what would be expected by this theory. In contrast, Figures 22 and 23 for the screens show the observed turbulence level significantly below that predicted by this theory at this location. This difference is probably due to the turbulence generated by the shear layer of the grid.

With the turbulence level of 1.5% at the simulated entrance to the Compressor Research Facility test article inlet, a contraction ratio must be used to obtain a turbulence level of less than 1%. From Batchelor[13], the contraction ratio based on area required to reduce the turbulence level from 1.5% to less than 1% would be 1.5 to 1. Therefore, in the full-scale facility, the largest allowable diameter bellmouth for a test article would be 2.48 meters which is larger than required to accommodate the maximum flow rate of the facility.

The turbulence decay for the remaining flow conditioning elements is shown in Figure 26 for 700 cm./sec. and Figure 27 for 1340 cm./sec. No theory is shown on these figures. However, if the theory is applied to the honeycomb configuration at 24.8 cm. downstream from the honeycomb, it is observed that the measured turbulence is less than what would be predicted by the theory, similar to the screens of Figures 22 and 23. On the other hand, if the theory is applied to the 1/2 grid, again at 24.8 cm. downstream from the grid, the measured

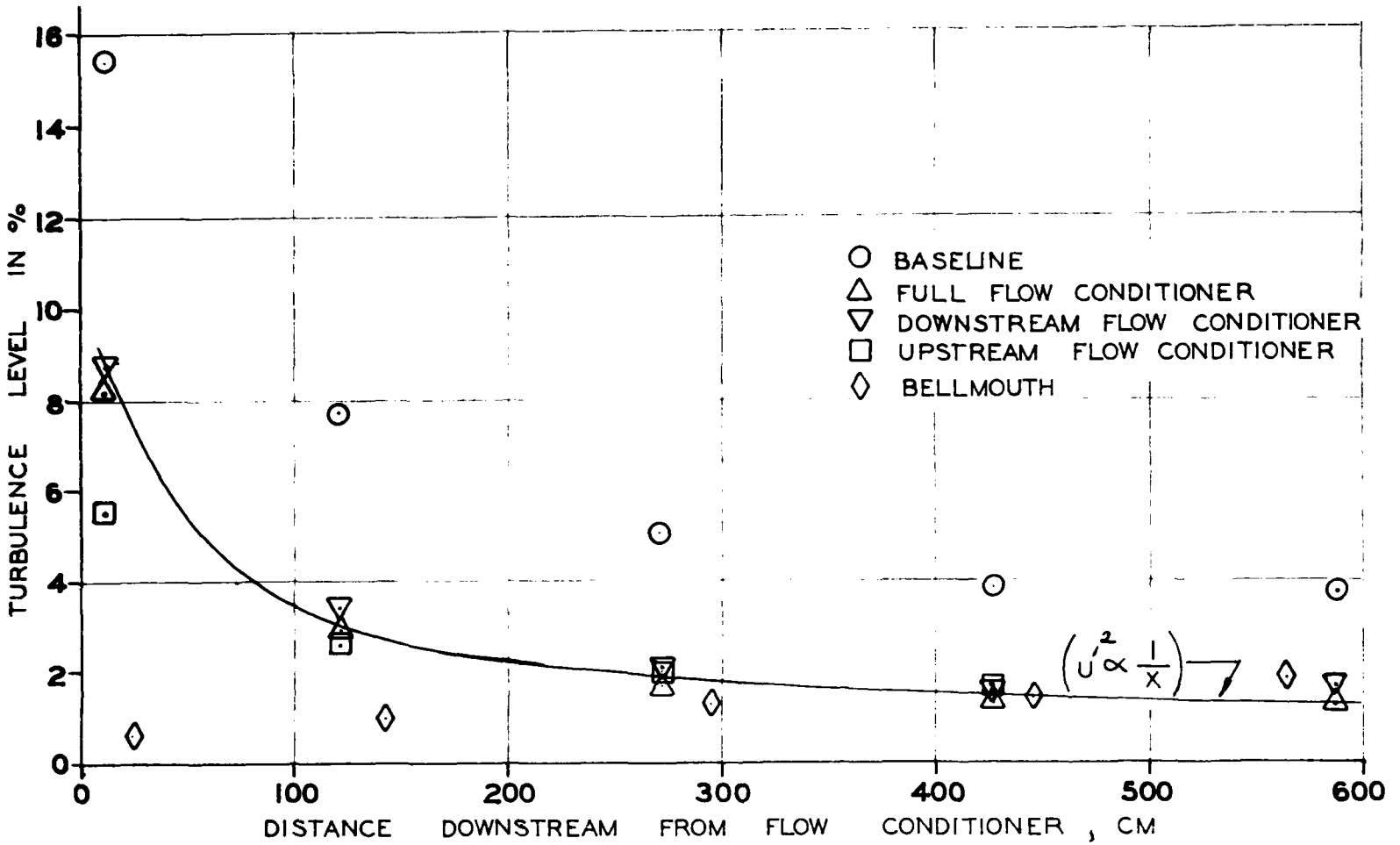

FIGURE 24 TURBULENCE DECAY DATA FOR FLOW CONDITIONERS AT 700 CM/SEC.

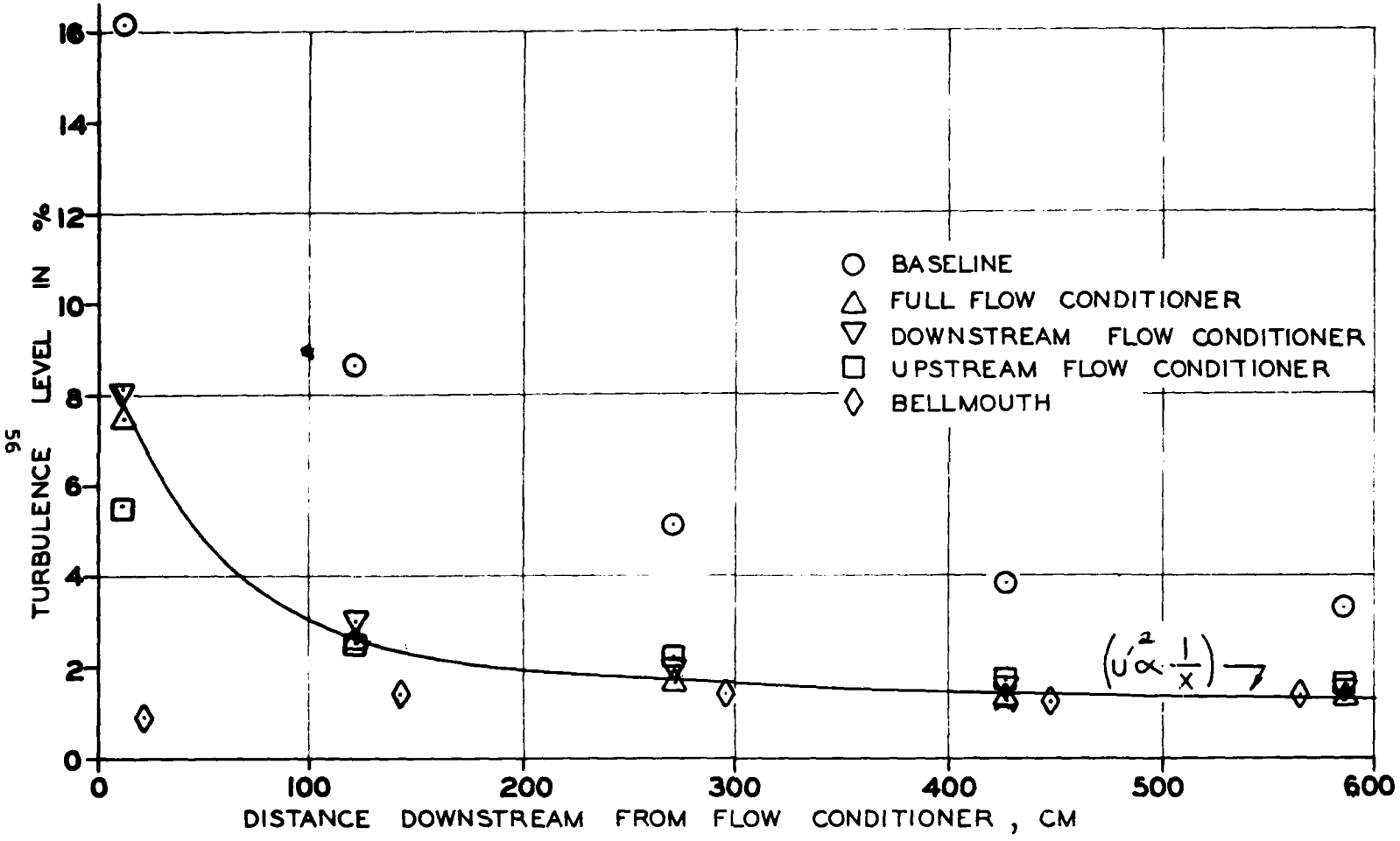

FIGURE 25 TURBULENCE DECAY DATA FOR FLOW CONDITIONERS AT 1340 CM/SEC.

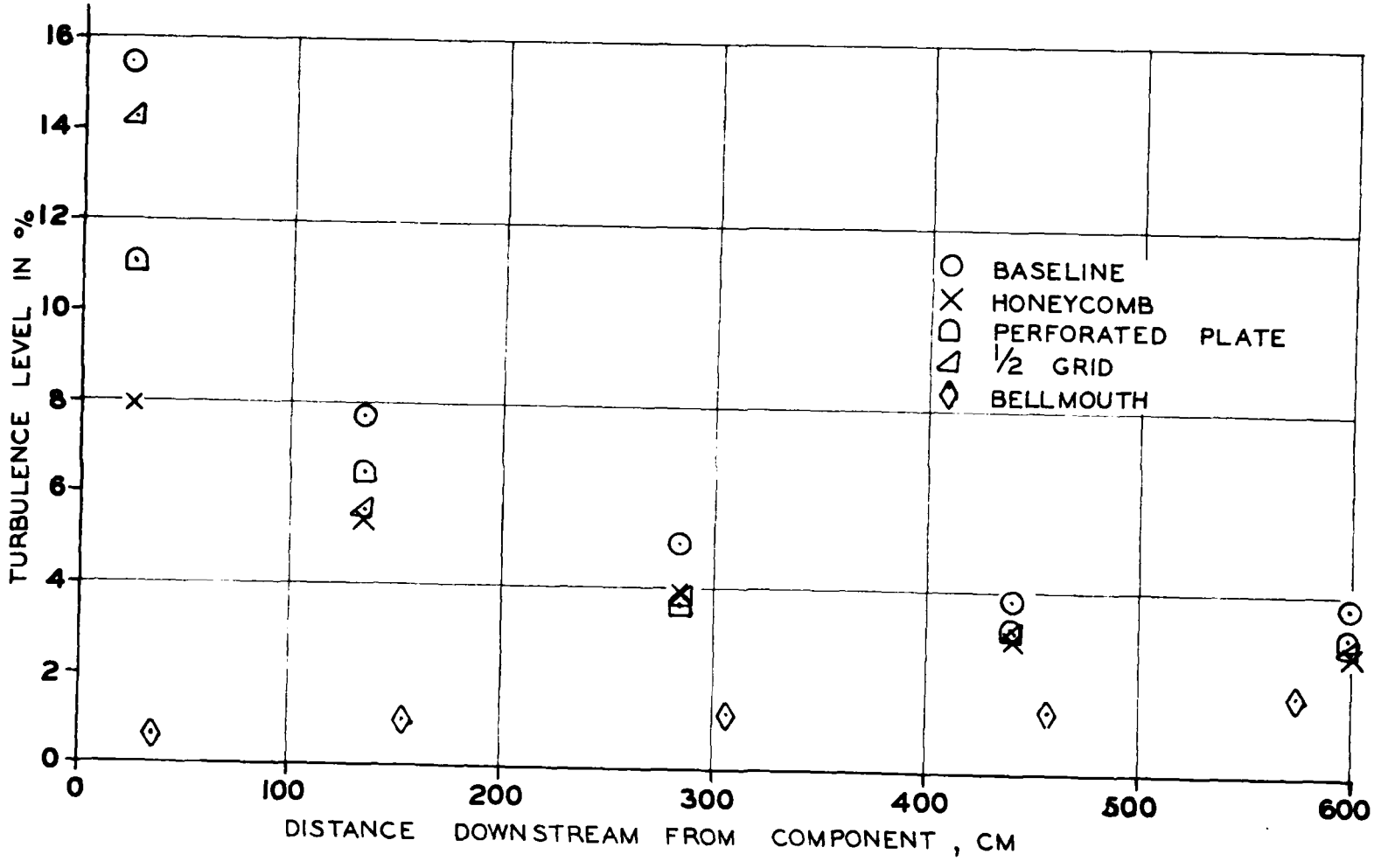

FIGURE 26 TURBULENCE DECAY DATA FOR RELATED COMPONENTS AT 700 CM/SEC.

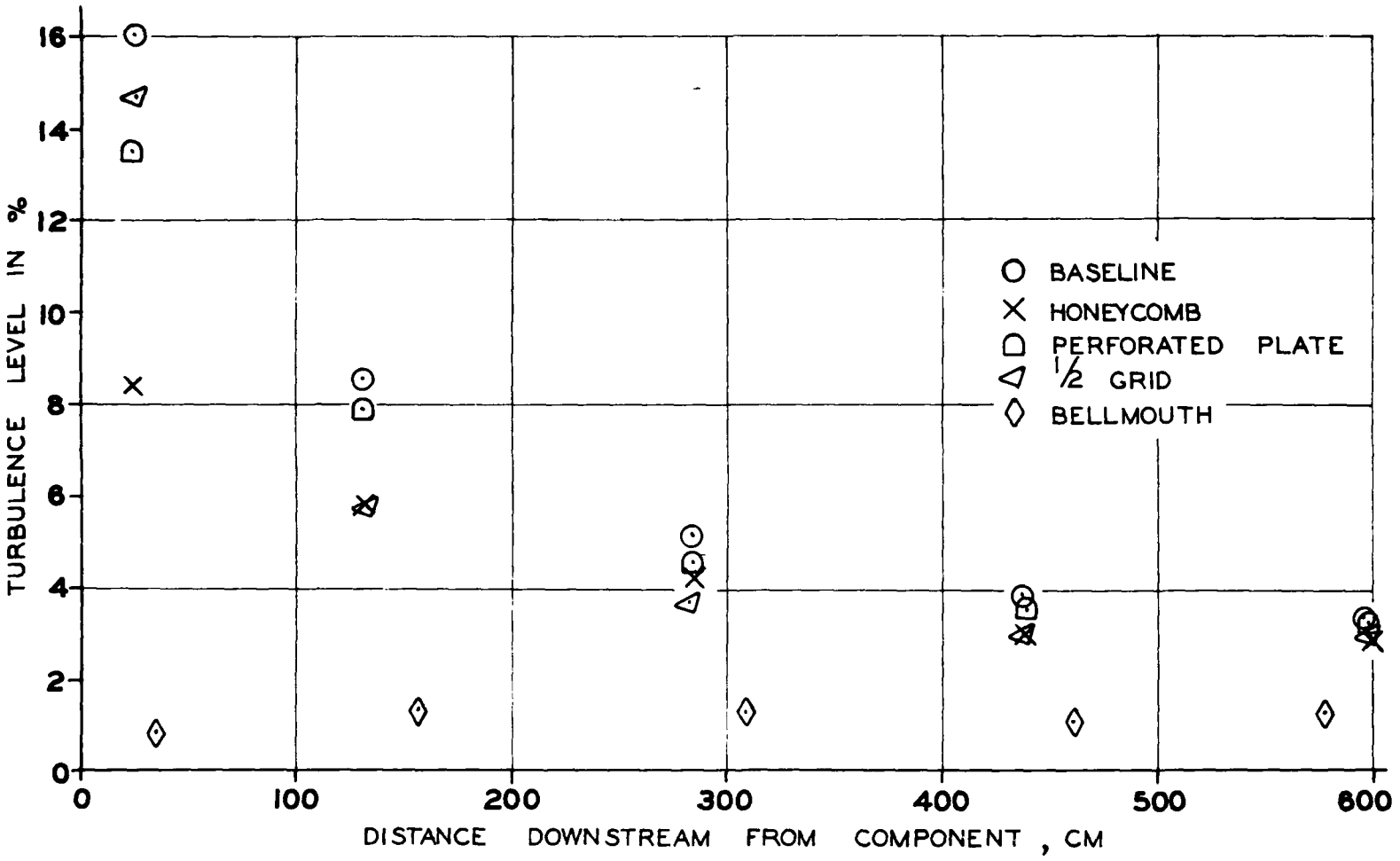

FIGURE 27 TURBULENCE DECAY FOR RELATED COMPONENTS AT 1340 CM/SEC

turbulence level is higher than the predicted level, similar to the full-flow conditioner of Figures 24 and 25. This effect substantiates the fact that the shear layer of the grid creates more turbulence than a screen or screen type element.

It should be noted that for the honeycomb structure, the parameter L in Equation (15) would be 2.5 to .8 for the velocity range in the Compressor Research Facility. This condition would indicate a highly developed flow and would probably counteract any of the effects of the upstream screen on turbulence reduction. Further, the full-flow conditioner probably behaves as one conditioning unit because the two individual units are not separated by a significant distance and the downstream honeycomb counteracts much of the turbulence reducing effects of the upstream conditioning unit. However, it should be noted that the flow conditioning system for the full-scale facility must meet other flow quality standards. Therefore, a judgement on the overall performance of the flow conditioning system cannot be made from this investigation alone.

VI. CONCLUSIONS AND RECOMMENDATIONS

1. From the data obtained in this work, it is concluded that the full-flow conditioner for the Compressor Research Facility will reduce the 40 to 60% of incoming turbulence level to less than 1% at the test compressor inlet. Therefore, from a turbulence level standpoint, the full-scale facility will be able to accurately establish test compressor characteristics within its design goals.

2. The turbulence behind any of the flow conditioning configurations tested decayed in a manner similar to the initial period of decay law reported in Reference 5. It is concluded that turbulence on the order of 10%, as in this experiment, will decay due to both inertia and viscous effects until the level of turbulence becomes on the order of 1%.

3. The turbulence reduction data for individual components obtained in this work correlates well with the theory of Dryden and Schubauer as applied in Reference 8. This agreement would tend to validate the approach taken to investigate turbulence decay for the flow conditioning system of the Compressor Research Facility.

4. From the data obtained in this experimentation, the turbulence reduction factor for the three flow conditioning configurations do not agree with the Dryden and Schubauer theory. It is concluded that this disagreement is a result of the interaction between the individual elements in these configurations.

5. From the results of this work, it can be concluded that the velocity profile within the honeycomb structure probably negates much

of the turbulence reducing effect of the upstream screen in a single conditioning unit. For the same reason, the honeycomb located in the downstream unit probably reduces much of the effects of the upstream unit in the full-flow conditioning configuration.

6. The interactions of the various components were not studied; however, as indicated above, these interactions are of great importance and should be studied.

7. Obviously, experiments of turbulence measurement on the full-scale facility are advantageous, and at this date they are being formulated. The validity of the present work and other small-scale experimentation conducted on the flow conditioning system will be determined by the experiments conducted in the full-scale facility.

REFERENCES

1. "An Assessment of Flow Quality Requirements for the Compressor Research Facility," G.D. Huffman, F.R. Ostdiek and R.B. Rivir, AFAPL-TR-75-75.

2. "Development of a National Compressor Research Facility," W. Mitchell, R. Martin, F. Ostdiek, R. Rivir and P. Shahady, AIAA/SAE 13th Propulsion Conference, Orlando, Florida, July 11-13, 1977.

3. "Compressor Research Facility Scale Model Flow Conditioning Results," F.R. Ostdiek, R.B. Rivir, AFAPL Memo, 22 July 1976, unpublished.

4. "Compressor Research Facility Aerodynamic Analysis," G.D. Huffman, AFAPL-TR-79-2021.

5. "Decay of Turbulence in the Initial Period," G.K. Batchelor and A.A. Townsend, Royal Society of London Proceedings, Series A, Vol. 193.

6. "Decay of Turbulence in the Final Period," G.K. Batchelor and A.A. Townsend, Royal Society of London Proceedings, Series A, Vol. 193.

7. "Aerodynamic Characteristics of Damping Screens," G.B. Schubauer, W.G. Spangenberg and P.S. Klebanoff, NASA TN 2001, January 1950.

8. "The Use of Damping Screens for the Reduction of Wind-Tunnel Turbulence," H.L. Dryden and G.B. Schubauer, Journal Aero Sciences, Vol. 14, No. 4, April 1947.

9. Boundary-Layer Theory, H. Schlicting, McGraw-Hill Series in Mechanical Engineering, 1968.

10. "The Effects of Turbulence on Laser Beam Quality," R.B. Rivir, AFAPL-TR-76-94.

11. Resistance Temperature Transducers, V.A. Sandborn, Metrology Press, 1972.

12. "Turbulence, Experimental Methods," S. Corrsin, Hanbuch Den Physik, S. Flugge and C. Truesdell, Volume VIII, Part 2, Springer-Verlag, 1963.

13. The Theory of Homogeneous Turbulence, G.K. Batchelor, Cambridge University Press, 1953.

*U.S.Government Printing Office: 1980 — 657-084/178